Highlights:

- Conceptual review of hyporheic zones of rivers as natural anoxic-oxic bioreactors

- Interactions between organohalide respiration and biogeochemical cycling

- Aerobic vinyl chloride mineralisation during hyporheic mixing is conceptualised

- Field experience, challenges and characterisation technologies critically reviewed

1   Natural attenuation of chlorinated ethenes in hyporheic zones: a review of

2   key biogeochemical processes and in-situ transformation potential

3   John J. Weatherill [a] *, Siavash Atashgahi [b], Uwe Schneidewind [c], Stefan Krause [d], Sami Ullah [d], Nigel

4   Cassidy [e], Michael O. Rivett [f g]

5   [a] School of Physical and Geographical Sciences, Keele University, UK. Current address: School of

6   Biology, Earth and Environmental Science, University College Cork, Ireland.

7   [b] Laboratory of Microbiology, Wageningen University & Research, Stippeneng 4, 6708 WE

8   Wageningen, The Netherlands.

9   [c] Department of Engineering Geology and Hydrogeology, RWTH Aachen University, Aachen,

10   Germany.

11   [d] School of Geography, Earth and Environmental Science, University of Birmingham, UK.

12   [e] School of Engineering, University of Birmingham, UK.

13   [f] Department of Civil and Environmental Engineering, University of Strathclyde, Glasgow, UK.

14   [g] GroundH$_2$O plus Ltd., Quinton, Birmingham, UK.

15   * Corresponding author: John Weatherill, School of Biology, Earth and Environmental Science,

16   University College Cork, Ireland. Email: john.j.weatherill@gmail.com.

17 **Abstract**

18   Chlorinated ethenes (CEs) are legacy contaminants whose chemical footprint is expected to

19 persist in aquifers around the world for many decades to come. These organohalides have been reported

20 in river systems with concerning prevalence and are thought to be significant chemical stressors in urban

21 water ecosystems. The aquifer-river interface (known as the hyporheic zone) is a critical pathway for

22 CE discharge to surface water bodies in groundwater baseflow. This pore water system may represent a

23 natural bioreactor where anoxic and oxic biotransformation process act in synergy to reduce or even

24 eliminate contaminant fluxes to surface water. Here, we critically review current process understanding

25 of anaerobic CE respiration in the competitive framework of hyporheic zone biogeochemical cycling

26 fuelled by in-situ fermentation of natural organic matter. We conceptualise anoxic-oxic interface

27 development for metabolic and co-metabolic mineralisation by a range of aerobic bacteria with a focus

28 on vinyl chloride degradation pathways. The superimposition of microbial metabolic processes

29 occurring in sediment biofilms and bulk solute transport delivering reactants produces a scale

30 dependence in contaminant transformation rates. Process interpretation is often confounded by the

31 natural geological heterogeneity typical of most riverbed environments. We discuss insights from recent

32 field experience of CE plumes discharging to surface water and present a range of practical monitoring

33 technologies which address this inherent complexity at different spatial scales. Future research must

34 address key dynamics which link supply of limiting reactants, residence times and microbial

35 ecophysiology to better understand the natural attenuation capacity of hyporheic systems.

36 **Keywords:** Chlorinated ethenes, hyporheic zone, natural attenuation, biogeochemistry,

37 biotransformation, heterogeneity.

38 **Abbreviations:**

39 1,1,1-TCA: 1,1,1-trichloroethane; DCA: 1,2-dichloroethane; Ac: acetate, CA: chlorinated ethane;

40 cDCE: *cis*-1,2-dichloroethene; CE: chlorinated ethene; Da: Damköhler number; DIC: dissolved

41 inorganic carbon; DNAPL: dense, non-aqueous phase liquid; DOC: dissolved organic carbon; DOM:

42 dissolved organic matter; DON: dissolved organic nitrogen; HCB: hexachlorobenzene; HCE: higher

43 chlorinated ethene; HFC: hyporheic flow cell; K: saturated hydraulic conductivity; LCE: lower

44 chlorinated ethene; OHR: organohalide respiration; OHRB: organohalide-respiring bacteria; OM:

45 organic matter; PCE: tetrachloroethene; PCR: polymerase chain reaction; POM: particulate organic

46 matter; SCFA: short chain fatty acid; SOM: sedimentary organic matter; TCE: trichloroethene; TCM:

47 trichloromethane; TEA: terminal electron acceptor; TEAP: terminal electron accepting process; VC:

48 vinyl chloride.

49 **1 Introduction**

50 Legacy soil and groundwater contamination by chlorinated ethenes (CEs) remains a global

51 environmental concern (Burston et al., 1993; Jackson, 1998; Rowe et al., 2005; Rivett et al., 2006, 2012;

52 2014). The higher CEs (HCEs), tetrachloroethene (PCE) and trichloroethene (TCE) are parent

53 compounds employed historically as non-polar solvents for industrial cleaning and degreasing

54 applications which enter aquifers as dense, non-aqueous phase liquids (DNAPLs) (Pankow and Cherry,

55 1996; Rivett et al., 2014) and release dissolved-phase plumes (e.g. Benker et al., 1996; Rivett and

56 Feenstra, 2005; Koch and Nowak, 2015). Diffusive retention of HCEs in low-permeability and fractured

57 formations is increasingly recognised as an important driver of plume longevity from the resulting back-

58 diffusive flux (Parker et al., 1994; Seyedabbasi et al., 2012; Damgaard et al., 2013; Yang et al., 2014).

59 Under predominantly anoxic conditions, HCEs are reductively transformed to the lower CEs (LCEs)

60 *cis*-1,2 dichloroethene (cDCE) and vinyl chloride (VC) (Squillace and Moran, 2007; Chambon et al.,

61 2010; Huang et al., 2014; Lu et al., 2015). CEs have been detected in surface water with alarming

62 frequency around the world (e.g. Christof et al., 2002; McGuire et al., 2004; Ellis and Rivett, 2007;

63 Yamamoto et al., 2014 Wittlingerová et al., 2016). Groundwater baseflow input of CEs has been

64 implicated as a contributory factor in the global impoverishment of surface water ecological quality

65 known as urban stream syndrome (Meyer et al., 2005; Roy and Bickerton, 2011; Roy et al., 2017). The

66 aquifer-river interface, inclusive of the hyporheic zone (Fig. 1) forms a key diffuse pathway for

67 discharge of groundwater plumes hydrologically connected with local surface water bodies (Table 1)

68 (Conant et al., 2004; Chapman et al., 2007; McKnight et al., 2012; Weatherill et al., 2014; Puigserver et

69 al., 2014; Simsir et al., 2017; Sonne et al., 2017).

70   The hyporheic zone of streams and rivers has been defined by various disciplines from alternative

71 perspectives (e.g. Boulton et al., 1998; Buss et al., 2009; Krause et al., 2011; Cardenas, 2015). In this

72 review, we conceptualise the hyporheic zone as a dynamic volume of the saturated zone where the pore

73 water domain is physically influenced by exchanges across the sediment–water interface (Cardenas,

74 2009). This spatially and temporally variable volume may encompass shallow benthic sediments and

75 adjacent parts of the alluvial aquifer (Boano et al., 2014). The transition zone is frequently heterogeneous

76 with a wide range of saturated hydraulic conductivities (K) and associated scaling of solute residence

77 times (Haggerty et al., 2002; Sawyer and Cardenas, 2009; Gomez-Velez et al., 2014). Fluvial sediments

78 are sites of organic matter (OM) retention with high interstitial surface area linked to enhanced microbial

79 metabolic activity and characterised by sharp physical and biogeochemical gradients (Krause et al.,

80 2013, 2014; Boano et al., 2014; Atashgahi et al., 2015; Narango et al., 2015; Briggs et al., 2016). A

81 generic scenario is depicted in Fig. 1 where OM present in the sediment sequence induces anoxia along

82 discharging groundwater flow paths through the interface. The CE plume depicted may be composed

83 solely of parent HCEs (e.g. McKnight et al., 2010) or a mixture of LCEs (e.g. Sonne et al., 2017; Rønde

84 et al., 2017). Shallow oxic zones are created where local hyporheic exchange flows with the river

85 penetrate the underlying anoxic zone (Hester et al., 2013; 2017, Trauth et al., 2014). Heterotrophic

86 biogeochemical cycling of carbon, nitrogen, sulfur and metals will take place along anoxic sediment

87 flow paths (Baker et al., 2000; Mermillod-Blondin et al., 2005; Lautz and Fanelli, 2008; Rahimi et al.,

88 2015). Fluvial sediments can form niche environments for anaerobic biotransformation of CEs by

89 reductive dechlorination and much interest has arisen in their intrinsic capacity to assimilate

90 groundwater CE loads in baseflow (Table 1) (Conant et al., 2004; Abe et al., 2009; Hamonts et al., 2009;

91 Weatherill et al., 2014; Atashgahi et al., 2015; Freitas et al., 2015; Simsir et al., 2017). Discharging

92   groundwater flow paths through fluvial sediments may enter into mixing zones around infiltrating

93   surface water during hyporheic exchange flows (Boano et al., 2014; Gomez-Velez et al., 2014; Hester

94   et al., 2017). Dynamic pore water oxygen (O_2) gradients are induced in mixing zones as a result (Trauth

95   et al., 2014; Vieweg et al., 2015; Cardenas et al., 2016). These mixing zones provide a separate niche

96   environment for aerobic mineralisation of LCE daughter products originating in the anoxic zone or in

97   partially dechlorinated plumes (e.g. Rønde et al., 2017). Hence, hyporheic zones of groundwater-fed

98   rivers may constitute a unique natural 'biobarrier' for complementary anaerobic and aerobic biological

99   treatment of diffuse baseflow CE pollution (Hamonts et al., 2007; Abe et al., 2009; Atashgahi et al.,

100   2017a; Simsir et al., 2017).

101   The aim of this review is to provide a critical evaluation of the current understanding of

102   synergistic anoxic-oxic biotransformation processes and their environmental supporting conditions in

103   typical riverbed sediment sequences. We consider the fate of parent HCEs in anaerobic heterotrophic

104   food webs driven by OM fermentation and observed metabolic interactions with key biogeochemical

105   cycles. We conceptualise the development of anoxic-oxic interfaces in surface water mixing zones

106   which support aerobic bacteria capable of assimilating LCEs via metabolic and cometabolic pathways

107   with a particular focus on VC. We discuss challenges in integrating microbially-mediated transformation

108   processes occurring in sediment biofilms with larger scale hydrological fluxes observable at field scale.

109   We critically review available in-situ monitoring technologies and support our discussions with insights

110   from recent field experience. This process-based understanding is intended to underpin the risk-based

111   management of legacy CE contamination. The coupled biogeochemical and transport processes

112   understanding is highly relevant for river restoration and prospective ecological engineering applications

113   aimed at reducing the impact of organohalide stressors in urban streams (e.g. Lawrence et al., 2013;

114   Rasmussen et al., 2016; Roy et al., 2017).

115   **2   Biotransformation of chlorinated ethenes in riverbed sediments**

116   Biotransformation of CEs in hyporheic zones will occur when requisite bacteria, a circumneutral

117   pH, nutrients and electron donors/acceptors are present and where solute residence time equals or

118   exceeds the transformation timescale (half-life) of the contaminant (Meckenstock et al., 2015). In anoxic

119 zones, CEs may undergo anaerobic reductive dechlorination (hydrogenolysis) by heterotrophic bacteria

120 where chlorine atoms are sequentially replaced by hydrogen (Fig. 2) in organohalide respiration (OHR)

121 (Vogel et al., 1987; Hug et al., 2013; Leys et al., 2013). LCEs produced by OHR may reach oxic

122 interfaces where metabolic and co-metabolic aerobic pathways lead to complete natural attenuation.

123 This part of our review profiles key advances in the understanding of these synergistic biotransformation

124 process for which hyporheic zones present a unique capacity.

125 **2.1 Organohalide respiration**

126 Under anoxic conditions, CEs are terminal electron acceptors (TEAs) for energy conservation

127 (Fig. 2) during oxidation of an electron donor (usually hydrogen) in the presence of a carbon source

128 (usually acetate) and a nitrogen source (ammonium) (Mohn and Tiedje., 1992; Smidt and de Vos, 2004).

129 OHR is an energy-conserving process where the chemically stable carbon-halide bond of organohalides

130 is unlocked by replacing the halogen atom with hydrogen and liberating it as a halide (Fig. 2) (Maymo-

131 Gatell et al., 1997; McCarty, 1997; Aulenta et al., 2002). The reductive cleavage of carbon-halide bonds

132 is catalyzed by membrane-bound, cobalamin-containing enzymes known as reductive dehalogenases

133 (Bommer et al., 2014). OHR is mediated by organohalide-respiring bacteria (OHRB) belonging to

134 district bacterial groups i.e., *Chloroflexi*, *Proteobacteria* and *Firmicutes* (Atashgahi et al., 2016).

135 Members of the genus *Dehalococcoides mccartyi, Dehalogenimonas* and *Dehalobacter* spp. are

136 restricted to OHR for their metabolism, although fermentative growth is also shown in the latter (Justica-

137 Leon et al., 2014; Lee et al., 2012; Yang et al., 2017). In contrast, *Geobacter*, *Desulfuromonas*,

138 *Anaeromyxobacter*, *Desulfomonile*, *Desulfoluna*, *Desulfovibrio*, *Sulfurospirillum* and

139 *Desulfitobacterium* genera are facultative OHRB with versatile metabolisms including but not restricted

140 to OHR (Maphosa et al., 2010; Atashgahi et al., 2016).

141 **2.2 Potential heterotrophic food webs in anoxic zones**

142 **2.2.1 Carbon flow in the hyporheic zone**

143 Dissolved organic matter (DOM) is a key source of electron donors and nutrients for OHR and

144 other heterotrophic terminal electron accepting processes (TEAPs) in hyporheic zones (Pusch and

145 Schwoerbel, 1994; Fischer et al., 2005; Zarnetske et al., 2011; Stegen et al., 2016). Anaerobic DOM

146 mineralisation is coupled to the reduction of TEAs as follows (Donn and Barron, 2013):

147 DOM + TEA $\rightarrow$ DIC + metabolite + NH_4

148 Where TEA (in descending potential metabolic energy yield) is $O_2 > NO_3 > PCE > Fe(III) > TCE >$

149 $cDCE > SO_4 > VC > CO_2$, DIC is dissolved inorganic carbon, metabolite is N_2, CO_2, Mn^{2+}, LCEs, Fe^{2+},

150 ethene, ethane, S^{2-}, CH_4 and acetate) and ammonium (NH_4). Biogeochemical cycling and OHR will take

151 place when DOM concentrations exceed the stoichiometric requirements (non-limiting) for each TEAP

152 where the reaction timescales are less than the exposure time along reactive sediment flow paths (Haest

153 et al., 2011; Zarnetske et al., 2012; Abbot et al., 2016). Hyporheic sediments are often enriched in

154 complex organic matter (Fig. 1) derived from allochthonous terrestrial ecosystem (such as soil particles

155 and leaf litter) and anthropogenic sources of dissolved-phase and suspended particulate material (e.g.

156 urban runoff and wastewater discharges) (Stelzer et al., 2014; Atashgahi et al., 2015). The nature of the

157 organic material that accumulates in riverbed sediments may also influence the effective residence time

158 of the plumes through hydrophobic partitioning to sedimentary organic matter (SOM) (Conant et al.,

159 2004; Allen-King et al., 2002; Wang et al., 2013).

160   Anaerobic decomposition of particulate organic matter (POM) is initiated by extracellular

161 hydrolytic enzymes produced by primary fermenters which release soluble DOM components capable

162 of traversing bacterial cell walls (Fig. 2) (Mani et al., 2016). Hydrolysis is frequently the rate-limiting

163 step in sedimentation zones with high POM loading rates, large particle size ranges or where highly

164 polymerised complex POM (e.g. lignin) are present that are not readily degradable (Gavala et al., 2003;

165 Nogaro et al., 2007; Atashgahi et al., 2014). DOM hydrolysis is a source of labile dissolved organic

166 carbon (DOC) and dissolved organic nitrogen (DON) species including organic acids and the soluble

167 oligomers and monomers of proteins and carbohydrates which influence the onset and rate of anaerobic

168 respiration processes (Jakobsen and Postma, 1999; Zarnetske et al., 2011; Mineau et al., 2013; Helton

169 et al., 2015). Groundwater typically contains <0.15 mM of DOC (Lapworth et al., 2009; Chapelle et al.,

170 2012). Of this, the labile fraction represents only 0.5–5% of carbon present which is often below

171 thresholds required for induction of catabolic genes (Egli, 2010). In contrast, hyporheic zone pore water

172 DOC concentrations often exceed 1 mM (e.g. Lewandowski and Nützmann, 2010) of which 10–30% is

173 labile and bioavailable (Baker et al., 1999; Vidon and Hill, 2004; Romani et al., 2006).

2.2.2 Molecular hydrogen

Free dissolved hydrogen (H_2) is produced from internal proton reduction during primary and secondary DOC fermentation (Fig. 2) (Nath and Das 2004; Hallenbeck et al., 2009). H_2 serves as the strict electron donor for known obligate OHRB (such as *D. mccartyi*) as well as many facultative OHRB (Jugder et al., 2016). A generalised reaction for H_2 production during fermentation of DOC is given as follows:

$$DOC + 2H_2O \rightarrow DIC + 2H_2 + SCFA + H^+$$
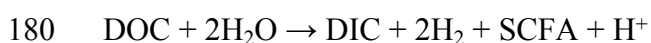
Where SCFA is a short-chain fatty acid which is discussed in the next section. In anoxic sediment zones, DOC fermentation is a metabolic process utilised by common fermentative bacteria such as *Desulfovibrio* (Walker et al., 2009), *Syntrophomonas* (Sieber et al., 2010), and *Clostridium* (Wu et al., 2012), among others. H_2 is also produced by homoacetogens (Diekert and Wohlfarth, 1994), certain acetoclastic methanogens (Heimann et al., 2007) and *Geobacter* spp. (Loffler and Sanford, 2005). Low extracellular H_2 concentrations are required for DOC fermentation to be energetically favourable. This is often maintained by unique syntrophic interspecies H_2 transfer relationships (Fig. 3) amongst anaerobes which express membrane-bound hydrogenases (Walker et al., 2009; Morris et al., 2013; Sieber et al., 2014; Jugder et al., 2015). As a result, the reaction timescales for H_2 uptake are typically on the order of minutes (Heimann et al., 2009). Under electron-donor limiting conditions, ambient H_2 concentrations in sediments are often at steady-state that is determined by the hydrogenotrophs with the lowest threshold concentration (Lovely and Goodwin, 1988; Fennel et al., 1997; Loffler et al., 1999; Hoelen and Reinhard, 2004). H_2 threshold ranges have been reported for specific TEAPs (Fig. 4) ranging from <0.1 nM for denitrification to >350 nM for homoacetogenesis. From Fig. 4 it can be observed that HCE reduction (0.6–0.9 nM) occurs at an overlapping H_2 threshold to Fe(III) reduction (0.1–0.8 nM) whereas LCE reduction overlaps with sulfate reduction and methanogenesis (Paul et al., 2016). Overlap of TEAP H_2 thresholds are commonly observed in experimental studies (e.g. Jakobsen and Postma, 1999; Aulenta et al., 2008; Paul et al., 2016) with lower levels than predicted from thermodynamic considerations (Heimann et al., 2009). This phenomenon has been attributed to kinetic effects arising from the relative efficiencies in H_2 producers and consumers in microbial consortia (Richardson, 2016).

2.2.3   Short chain fatty acids

Short-chain fatty acid (SCFAs) are labile DOC species such as butyrate, propionate and lactate produced as intermediates during primary DOC fermentation (Fig. 2) and are accompanied by an increase in pore water H^+ ion concentrations. SCFAs readily undergo secondary fermentation to produce electron donors (Giovannini et al., 2016). SCFA turnover is often the rate-limiting step in the anaerobic decomposition of complex DOM (Mani et al., 2016) and release of reducing equivalents for OHRB and other heterotrophs (Atashgahi et al., 2014). The most frequently reported SCFA in hyporheic zones is acetate which is both a terminal metabolite and intermediate of DOC fermentation (Fig. 2) (Baker et al., 1999; Baker and Vervier, 2004; Hlaváčová et al., 2005). It is an easily assimilated carbon source and possible direct electron donor for OHRB which may be independent of extracellular H_2 (Richardson, 2016). Under high pore water H_2 concentrations (>350 nM) acetate is also produced from other labile DOC compounds (i.e. methanol) or H_2/CO_2 by homoacetogens such as *Acetobacterium*, *Sporomusa*, *Spirochaeta* (Ziv-El et al., 2012).

Acetate has been widely shown to sustain respiration of HCEs as far as cDCE by facultative OHRB groups such as *Geobacter* and *Desulfuromonas* (Sharma and McCarty, 1996; Krumholz et al., 1996; Loffler et al., 2000; Wagner et al., 2012). For example, in contaminated aquifer media, Lee et al. (2007) found that whilst H_2 could sustain dechlorination of PCE as far as ethene, with uptake of acetate, dechlorination stalled at cDCE and proceeded at less than half the rate of H_2 alone. However, the role of acetate in OHR appears to be more complex. He et al. (2002) found that several organohalide-containing sediment microcosms amended with acetate alone were capable of sustaining PCE dechlorination to ethene. Their findings suggest a potential syntrophic partnership between cDCE and VC dechlorinators and acetate-oxidising bacteria (such as *Clostridium ultunense*) because of the low H_2 concentrations maintained by OHRB. Wei and Finneran (2013) also showed that acetate could sustain TCE, cDCE and VC dechlorination to ethene. Little difference in dechlorination rates were observed between amendments with 10 times more acetate. Similarly, higher production of acetate from solid organic polymeric materials used to stimulate cDCE in riverbed sediment microcosms did not lead to higher dechlorination rates as the excess organic loading was channelled to methanogenesis (Atashgahi et al., 2014). These results highlight the complex role acetate plays in anaerobic food webs with

229   sometimes contradictory effects observed in relation to OHR rates.

2.3   Interactions between OHR and alternative anaerobic TEAPs

231   Interspecies H_2 transfers between fermenters and anaerobic TEAPs (Fig. 3) including denitrification,

232   metal reduction, sulfate reduction and methanogenesis (Fig. 4) may influence the rate and extent of OHR

233   in anoxic zones (Aulenta et al., 2007). Toxic metabolites generated may also inhibit steps of the

234   dechlorination process (Berggren et al., 2013). In this section, we review the current understanding of

235   these competitive interactions between OHR steps and biogeochemical cycling in the hyporheic zone.

2.3.1   Nitrate reduction

237   Groundwater nitrate has become elevated over the last century as a result of the 6.4-fold increase

238   in global inorganic fertiliser production between 1961 and 1999 (Peng et al., 2002). Heterotrophic

239   denitrification producing nitrous oxide (N_2O) or dinitrogen (N_2) and dissimilatory nitrate reduction to

240   ammonium (NH_4) occur in suboxic conditions (<125 μM O_2) with ambient H_2 levels (<0.1 nM) which

241   are below the level at which OHR becomes favourable for HCEs (~0.6 nM) (Fig. 4). Nitrate respiration

242   has only a slightly lower energy yield than that of oxygen with reaction timescales in the order of hours

243   to days (Rivett et al., 2008a; Jahangir et al., 2012) and has been widely documented in hyporheic

244   sediments (e.g. Ullah et al., 2014; Heppell et al., 2014). The interactions between OHR and nitrate

245   respiration is apparently complex. Yu et al. (2014) have shown that nitrate stimulated OHR of

246   pentachlorophenol at concentrations below 1 mM (likely by providing OHRB with a nitrogen source for

247   growth) but became inhibitory at concentrations greater than 1 mM. This was supported by Chen et al.

248   (2002) where 3 mM of nitrate inhibited hexachlorobenzene respiration under lactate-fermentation

249   conditions in river sediments. Nelson et al. (2002) found PCE reduction inhibition from only 0.6 mM of

250   nitrate and sulfate in a mixed culture where H_2 was continuously fed at non-limiting aqueous

251   concentrations (0.4–0.8 mM). In that study, the metabolite N_2O was found to be an inhibitor of OHR at

252   13 μM. These results are consistent with capture of available electrons by denitrifiers and reduction of

253   ambient H_2 levels below the minimum threshold necessary for OHRB as a key inhibition mechanism

254   which is also in line with thermodynamic predictions and observed H_2 thresholds (Fig. 4).

2.3.2 Iron(III) reduction

Iron oxides and oxyhydroxides such as haematite (Fe_2O_3) and goethite ($FeO(OH)_3$) are abundant primary and secondary minerals in streambed sediments which contain Fe(III) as a solid or colloidal phase (Liu et al., 2014). Similarly, manganese oxide minerals such as pyrolusite (MnO_2) contain the TEA Mn(IV) which behaves comparably to Fe(III) in redox processes (Ng et al., 2016). Some facultative OHRB including *Desulfuromonas michiganensis* and *Geobacter lovleyi* (Sung et al., 2006) can also use Fe(III) as a TEA. Dissimilatory Fe(III) reduction to Fe(II) has been observed at a similar H_2 threshold range (0.1–0.8 nM) to HCE reduction (Fig. 4) and direct competition for electron equivalents is therefore possible over reaction timescales measured months. Inhibition of TCE reduction as a result of Fe(III) was demonstrated in microcosm studies prepared from dolomite aquifer materials (Yager et al., 1997). Dupont et al. (2003) observed general inhibition of TCE reduction due to a large pool of bioavailable Fe(III) minerals in microcosms prepared from contaminated aquifer sediment. In contrast, Wei and Finneran (2011) demonstrated simultaneous reduction of TCE to ethene and Fe(III) to Fe (II) in microcosms dominated by *D. mccartyi* and *Geobacter* with an excess of electron donor. Fe(III) was observed to facilitate OHR by maintaining the ambient H_2 concentration at a level favourable for the OHRB. Using the 'KB-1' organohalide-respiring enrichment culture (Duhamel et al., 2002), Paul et al. (2013) showed that pH and iron mineral structure play an important role in inhibition of OHR in assays of 14 different synthetic Fe(III) minerals using an excess of formate as an electron donor. High-surface area, poorly crystalline minerals (such as ferrihydrite) have a greater Fe(III) fraction which is bioavailable for electron transfer than highly crystalline minerals such as haematite and goethite. These studies suggest the inhibition of OHR by Fe(III) in hyporheic sediments is complex and will be strongly linked to pH, specific bioavailable iron mineral composition, surface area and sediment particle size rather than total sediment Fe(III) content (Paul et al., 2013; 2016).

2.3.3 Sulfate reduction

Sulfate is a major oxyanion in groundwater derived from chemical denudation of sedimentary rocks, oxidation of sulfide minerals and anthropogenic point sources. Dissimilatory sulfate reduction to sulfide occurs at similar observed H_2 thresholds (1–15 nM) to HCE and LCE respiration (Fig. 4). The presence of sulfate has been widely implicated where incomplete dechlorination leads to the

283 accumulation of LCEs (e.g. Bagley and Gossett, 1990; Pavlostathis and Zhuang, 1993; Lorah et al.,

284 2007) although laboratory studies of interactions between sulfate reduction and OHR are inconclusive.

285 For example, sulfate reduction was reported to affect rates of VC respiration and to a lesser extent cDCE

286 respiration (Boopathy and Peters, 2001; Aulenta et al., 2008; Pantazidou et al., 2012). Hoelen and

287 Reinhard (2004) observed respiration of TCE at sulfate concentrations of 1–2.6 mM in sediment

288 microcosm containing CEs and alkyl benzenes. TCE reduction was found to inhibit sulfate reduction

289 under an ambient H_2 concentration of 0.7 nM. Sulfate reduction at higher H_2 levels (2.5 nM) was

290 observed to compete with reduction of cDCE and VC which was sustained at a H_2 concentration of 1.6

291 nM. With constant H_2 concentrations (2–4 nM) sustained by lactate fermentation, Berggren et al. (2013)

292 found that the addition of sulfate affected the cDCE to VC respiration step the greatest (67%) in

293 comparison to VC to ethene (25%) and TCE to cDCE (8%). This work showed that sulfate addition

294 could produce a shift in the community structure of *D. mccartyi* leading to a reduction in OHR rates. In

295 contrast, an absence of any inhibitory effect under non-limiting electron donor conditions were shown

296 (e.g. Hoelen et al., 2006; Aulenta et al., 2007) and even sulfate addition was reported to strongly enhance

297 TCE respiration (Harkness et al., 2012). This may be a result of syntrophic partnership between sulfate

298 reducers and OHRB through provision of essential nutrients such as corrinoids (Men et al., 2012, Sutton

299 et al., 2015; Lu et al., 2017 Atashgahi et al., 2017a). A recent study on isolates, constructed consortia

300 and enrichments containing *D. mccartyi* showed that rather than sulfate, sulfide inhibited the growth of

301 *D. mccartyi* and its syntrophic partner, *Syntrophomonas wolfei* (Mao et al., 2017). Interestingly, in a co-

302 culture of *D. mccartyi* and sulfate-reducing *Desulfovibrio vulgaris* Hildenborough, a high sulfate

303 concentration (5 mM) was not inhibitory to OHR under electron donor (lactate) limitation likely due to

304 strong electron scavenging capacity of *D. mccartyi*. Moreover, at low sulfate levels (2 mM), sulfate

305 reduction was not inhibitory even under excess of electron donor (Mao et al., 2017).

306 **2.3.4 Methanogensis**

307 Methanogenesis represents the final phase of anaerobic DOM metabolism (Figs 2 and 4) with

308 methane production timescales in riverbed sediments reported in the order of 200 days (Sela-Adler et

309 al., 2017). Its importance as a metabolic process in hyporheic zones is becoming increasingly recognised

310 (e.g. Sanders et al., 2007; Shelley et al., 2014; Brablcová et al., 2015). Methanogens are dependent on

311 the same key substrates and electron donors as OHRB including acetate (via acetoclastic

312 methanogenesis) and H_2 (through hydrogenotrophic reduction of CO_2). The effects of acetoclastic

313 methanogenesis on OHRB is less well understood than hydrogenotrophic methanogenesis. Heimann et

314 al. (2006) suggested that acetoclastic methanogenesis may enhance VC dechlorination by providing

315 additional H_2 during acetate cleavage. The observed H_2 thresholds for hydrogenotrophic methanogenesis

316 (5–100 nM) are considerably greater than OHR (0.1–2.5 nM) (Paul et al., 2016) and OHRB have been

317 shown to out-compete hydrogenotrophic methanogens for reducing equivalents at low H_2 concentrations

318 (Ballapragada et al., 1997; Yang and McCarty, 1998; Azizian et al., 2010). CEs on the other hand have

319 been shown to have direct inhibitory effect on methanogenesis through enzyme inactivation although

320 the effect is less pronounced than for other organohalides such as chlorinated methanes (Chan and

321 Radom, 2011). Yu and Smith (2000) found that 137 μM of TCE could inhibit methanogenesis but no

322 effect was observed from PCE at 87 μM. In enrichment cultures containing fermenters, *D. mccartyi*

323 strain 195, homoacetogens and methanogens, Men et al. (2013) found that 22 μM of TCE caused

324 inhibition of hydrogenotrophic methanogenesis with an increase of electron flow to OHR by an average

325 of 7% under non-limiting H_2 concentrations (7–12 nM). Their results suggested that TCE could inhibit

326 homoacetogenesis at H_2 levels well above the optimal range for OHRB. That study showed that non-

327 methanogenic cultures generated significantly more ethene faster than methanogenic cultures and

328 suggested that fermenters (*Clostridium* spp.) may also supply essential nutrients (corrinoids) in addition

329 to H_2.

330 **2.3.5   Co-mingled organohalides**

331 An important consideration in the anaerobic transformation potential of hyporheic zones for CEs

332 is the presence of other organohalides in co-mingled groundwater plumes. The chlorinated ethane 1,1,1-

333 trichloroethane (1,1,1-TCA) introduced as an alternative to TCE and the chlorinated methane,

334 chloroform, (TCM) are frequent co-contaminants (Scheutz et al., 2011; Simsir et al., 2017). TCM is also

335 produced from natural processes in soils at low concentrations (<10 μM) (Laturnas et al., 2002). Both

336 1,1,1-TCA and TCM have been implicated in the accumulation of LCEs and VC in particular (Duhamel

337 et al 2002; Chung and Rittmann, 2008; Chan et al., 2011). TCM has also shown to inhibit dechlorination

338 of cDCE by *D. mccartyi*. (Maymo-Gatell et al., 2001). Conversely, Grostern et al. (2009) showed that

339   VC and cDCE to lesser extent can cause inhibition in the respiration of chlorinated ethanes (CAs) (1,1,1-

340   trichloroethane and 1,1-dischloroethane) Mayer-Blackwell et al. (2016) found that prolonged exposure

341   to 1,2-dichloroethane (DCA) in a VC-respiring culture caused selective changes in *D. mccartyi*

342   community structure and reduced VC-respiration capacity. Strong inhibition of DCA respiration was

343   observed by cDCE. At field scale, Simsir et al. (2017) observed no inhibitory effect on the CE

344   dechlorination capacity of hyporheic sediments due to the spatial segregation of CE and CA

345   dechlorinators (demarcated by expression of the *cfrA* gene associated with CA respiration) along

346   discharging groundwater flow paths. CEs themselves may also competitively inhibit steps of the OHR

347   sequence (Chambon et al., 2013). In a kinetic study using two mixed anaerobic cultures, Yu et al. (2005)

348   found that HCEs generally inhibited the respiration of LCEs whilst the LCEs weakly inhibited the

349   dechlorination of the HCEs. These studies highlight the complex inter-relationship between different

350   organohalide respiration steps and their metabolites.

351   **2.4   Development and implications of anoxic-oxic interfaces**

352   The higher halogen substitution of HCEs produces electrophilicity with resistance to electrophilic

353   attack by oxygenase enzymes of aerobic bacteria. Thus, oxidation of the carbon backbone of the ethene

354   molecule is energetically unfavourable (Vogel et al., 1987). Schmidt et al. (2014) recently reported

355   aerobic TCE oxidation as a sole carbon source which may be evidence of a novel metabolic process not

356   witnessed before. Nonetheless, susceptibility to the reductive pathway decreases proportionately with

357   the ratio of chlorine to carbon substituents. As such, LCEs may be amenable to transformation via

358   aerobic mineralisation pathways during hyporheic exchange flows (Atashgahi et al., 2013). From a

359   natural attenuation perspective, mineralisation reactions are attractive in that no stable toxic

360   intermediates generated (Tiehm and Schmidt, 2011).

361   **2.4.1   Hyporheic oxygen gradients and mixing zones**

362   A unique feature of hyporheic zones is the establishment of oxic domains located where river water

363   infiltrates bringing dissolved O_2 into riverbed pore water at saturation concentrations (Knapp et al.,

364   2015). A common scenario illustrating development of a shallow oxic zone within a predominantly

365   anoxic groundwater regime is depicted in Fig. 5 based on the conceptual framework of Figs 1 and 2. In

366   this situation, river water advection is induced by bed topography in a process known as hyporheic

367   exchange flow where water currents infiltrate on the upstream side of a topographic feature

368   (downwelling zone) and return back to surface water a short distance downstream along with

369   groundwater discharge (upwelling zone) (Harvey and Bencala, 1993; Gomez-Velez et al., 2014; Trauth

370   et al., 2015). These bi-directional hyporheic flow cells (HFCs) will develop at various scales around bed

371   and channel topographic features such as gravel bars, riffles, weirs, debris dams and meanders (Krause

372   et al., 2014; Boano et al., 2014; Fox et al., 2014).

373   A thin mixing zone (Fig. 5); governed by dispersive processes is thought to develop along the

374   boundary between HFCs and the surrounding groundwater-dominated pore water regime which is

375   characterised by unidirectional vertical and lateral flow paths (Zarnetske et al., 2012; Briggs et al., 2013;

376   Binley et al., 2013; Boano et al., 2014). Numerical simulations of conservative tracer transport through

377   hydrologically gaining hyporheic zones (Hester et al., 2013) have suggested that the thickness of this

378   mixing zone is greatest with homogeneous high K sediment (e.g. well-sorted sand or gravel) and reduced

379   groundwater discharge (Fig. 5). Conversely, in zones of elevated groundwater discharge, low stream

380   velocity and smooth bed topography the mixing zone may be reduced or absent entirely (Trauth et al.,

381   2015). During high river flows, HFCs and associated mixing zones may transiently penetrate into deeper

382   sediment layers which is accompanied by a temporary surface water invasion of the groundwater regime

383   at depth (e.g. Cuthbert et al., 2010; Hamonts et al., 2012; Byrne et al., 2013; Freitas et al., 2015). These

384   transient flow events may be particularly acute for urban rivers where peak flows are accentuated by

385   impervious catchment areas and channel canalisation (Meyer et al., 2005).

386   Advection of river water solutes including O_2 and DOM into bed sediments induces zones of

387   aerobic respiration (Fig. 5) where the reaction timescale is often rapid with zero-order rates reported

388   from 9 and 75 µM/h in a gravel bar (Vieweg et al., 2016). Where mixing occurs, an anoxic-oxic interface

389   will develop which shifts dynamically in response to the balance of surface water downwelling and

390   groundwater discharge pressures. Approximately 0.25–0.33 mM of DOC is required to deoxygenate

391   downwelling river water and other reductants from the anoxic zone (Fig. 4) such as Fe(II) and reduced

392   sulfur species may also consume O_2. Hence, conditions for a spatially fluctuating 'reactive fringe'

393 (Trauth et al., 2014) where complementary aerobic co-metabolic or growth-coupled assimilation of

394 cDCE and VC may be favoured. As a result, hyporheic zones can offer a spatially variable secondary

395 aerobic 'treatment' zone facilitating complete mineralisation of LCE metabolites (Atashgahi et al., 2013;

396 2017a).

397 **2.4.2 cDCE mineralisation**

398 Although cDCE is amenable to aerobic biotransformation, cDCE oxidation is not widely reported.

399 Bradley and Chapelle (1998a) were among the first to examine the potential for aerobic cDCE

400 mineralisation in microbial communities indigenous to riverbeds. Their study demonstrated biological

401 aerobic mineralisation of [^{14}C]-DCE (4:1 *cis*-to-*trans* isomers) to CO_2 in microcosms with recovery of

402 [^{14}C]-CO_2 ranging from 17–100% after just eight days. However, this study used natural sediment media

403 potentially containing a range of other substrates where co-metabolic processes could not be ruled out

404 (Bradley and Chapelle, 2000). Other work has shown aerobic cDCE mineralisation to proceed much

405 more slowly in aquifer media e.g. Klier et al. (1998) where just 3−10% mineralisation was achieved

406 after 180 days incubation. Moreover, Abe et al. (2009) found no evidence of cDCE removal in aerobic

407 riverbed microcosms incubated over 1.5 years. Such patchy metabolic cDCE aerobic degradation is

408 illustrated by the fact that only a single isolate, *Polaromonas* sp. JS666 has unequivocally shown to

409 grow by cDCE assimilation as the sole carbon and energy source (Coleman et al., 2002). With the advent

410 of compound-specific stable isotope analysis (CSIA), kinetic isotope fractionation of carbon (δ^{13}C-

411 cDCE) has provided an additional line of evidence that cDCE mineralisation may be a growth-linked

412 assimilatory process. Reported δ^{13}C enrichment factors for aerobic uptake of cDCE range from −7.1‰

413 to −22.4‰ for both mixed and pure cultures (Tiehm et al., 2008; Abe et al., 2009; Schmidt et al., 2010).

414 Biomass yields from cDCE uptake are reported to range from 6.1 to 12.5 g/M cDCE (Coleman et al.,

415 2002; Schmidt et al., 2010).

416 **2.4.3 VC mineralisation**

417 VC mineralisation is the most thermodynamically attractive CE oxidation process due to the

418 presence of only one chlorine substituent. Reaction timescales tend to be relatively rapid as a result. In

419 a radiolabelled microcosm study prepared from riverbed sediments (Bradley and Chapelle, 1998a), it

420   was shown that greater than 90% of VC was consumed after 12 days over a concentration range of 0.2

421   – 57 µM with uptake rates most adequately described by Michaelis-Menten kinetics. Bacteria capable

422   of aerobic VC oxidation as a sole carbon and energy source belong to a range of genera associated with

423   aerobic ethene assimilation (Mattes et al., 2010; Atashgahi et al., 2017a). Aerobic degradation of VC

424   and ethene are initiated by an alkene monooxygenase (EtnABCD) and an epoxyalkane-coenzyme

425   enzyme (EtnE) (Mattes et al., 2010). Various isolates have been identified including *Mycobacterium*

426   (Hartmans et al., 1985; Hartmans and DeBont, 1992; Fullerton et al., 2014; Le and Coleman, 2011),

427   *Pseudomonas* (Verce et al., 2000; 2001; Atashgahi et al., 2017a), *Ochrobactrum* (Danko et al., 2004,

428   Atashgahi et al., 2017a), *Nocardioides* (Coleman et al., 2002) and a *Ralstonia* (Elango et al., 2006).

429   Besides these classical VC-assimilators, stable isotope probing coupled to high-throughput 16S rRNA

430   gene sequencing and quantitative polymerase chain reaction (qPCR) extended the potential range of VC

431   assimilators to *Sediminibacterium*, *Aquabacterium*, *Variovorax*, *Brevundimonas*, *Tissierella*, and

432   *Rhodoferax*. (Paes et al., 2015; Wilson et al., 2016). Gossett (2010) found that biological VC respiration

433   could be sustained by *Mycobacterium* at extremely low (microaerophillic) extracellular O_2

434   concentrations (e.g. 0.3–0.6 µM). This finding raises the important question as to whether anoxic

435   conditions classically defined by O_2 concentrations less than 3 µM (Chapelle and McMahon, 2006) are

436   in fact still capable of supporting aerobic metabolism. Microaerophilic VC oxidation may also play a

437   role in the apparent 'stalling' of the dechlorination sequence at cDCE. A lack of VC detection may in

438   fact reflect scenarios where VC mineralisation rates equal or exceed the production rate under hypoxic

439   conditions (Bradley and Chapelle, 2011). In a recent microcosm study by Fullerton et al. (2014) subject

440   to inadvertent O_2 contamination, VC disappearance was observed without ethene formation. A strictly

441   aerobic *Mycobacterium* was identified in high numbers in the groundwater microcosm which was

442   inadvertently exposed to O_2. Atashgahi et al. (2013, 2017a) used 16S rRNA of *D. mccartyi* and genes

443   encoding for reductive dehalogenase enzymes (*vcrA* and *bvcA*) and the genes *etnC* and *etnE* involved in

444   aerobic mineralisation of VC and ethene to track the fate of VC in microcosms prepared from riverbed

445   sediments obtained from anoxic-oxic interface. Using a combination of chemical analysis and qPCR,

446   the authors demonstrated co-occurrence and co-activity of aerobic VC degraders and anaerobic *D.*

447   *mccartyi* in hyporheic sediments of the eutrophic Zenne River in urban Belgium (Atashgahi et al.,

448   2017a).

2.4.4   Aerobic co-metabolism

450   CEs can be transformed under aerobic conditions by co-metabolic reactions initiated by common

451   enzymes produced by a wide range of aerobes (Arp, 1995). No known benefit is gained through

452   acquisition of metabolic energy or biomass production (Horvath 1972; Wacket, 1988; Semprini et al.,

453   1994). Co-metabolism is a widespread process by microbes containing non-specific monooxygenase or

454   dioxygenase enzymes which catalyze the initial step in oxidation of a growth-supporting substrate in the

455   presence of O_2 (Suttinun et al., 2013). A lack of enzyme specificity leads to competition between CEs

456   and growth-supporting substrates for active sites of oxygenases leading to incorporation of O_2 into the

457   chloroethene molecule via reactive epoxide formation (Mattes et al., 2010). TCE, cDCE and VC are all

458   amenable to co-metabolic aerobic oxidation by the action of oxygenases. PCE was originally thought to

459   be recalcitrant to aerobic oxidation under environmental conditions, however it is shown to be

460   degradable by the enzyme toluene-o-xylene monooxygenase (Ryoo et al., 2000; Shim et al., 2001).

461   In hyporheic sediments, methane and ammonium are often the most abundant potential substrates

462   for co-metabolism produced from the in-situ anaerobic decomposition of DOM (Figs 2 and 5) (Donn

463   and Barron, 2013; Atashgahi et al., 2013; Brablcová et al., 2015; Simsir et al., 2017). Extensive

464   hyporheic methanotrophy has been documented in association with fine-grained sediments under

465   vegetation stands in streams (Sanders et al., 2007) and in well-oxygenated coarse-grained sediments

466   (Trimmer et al., 2010). The enzyme methane monooxygenase is produced by the methanotroph

467   *Methylosinus trichosporium* and has been shown to oxidise TCE, cDCE, VC and ethene (Oldenhuis et

468   al., 1991; Forrester et al., 2005; Findlay et al., 2016). Conrad et al. (2010) observed evidence of co-

469   metabolic TCE oxidation at field-scale in a contaminated aquifer with an increase in *M. trichosporium*

470   abundance accompanied by a decline in TCE and dissolved methane concentrations. A co-metabolic

471   process was verified in a supporting microcosm study prepared from aquifer media and isotopically-

472   labelled TCE (^{13}C-TCE). Simsir et al. (2017) presented evidence of possible hyporheic zone co-

473   metabolism with declines in cDCE and VC associated with strong vertical methane gradients (Fig. 6)

474   although no O_2 data are presented for comparison. Their study also documented the presence of

475   methanotrophs (*Methylococcaceae* spp.) coincident with the change in methane concentrations in the

476   sediment sequence. Nitrifying bacteria which oxidise ammonium produced from DOM metabolism (Fig.

477   2) such as *Nitrosomonas europaea* can also inadvertently oxidise TCE and LCEs (Arciero et al., 1989;

478   Vannelli et al., 1990; Rasche et al., 1991; Kocamemi and Cecen, 2005). Nitrification is well documented

479   in association with hyporheic flow cells (Jones, 1995; Briggs et al., 2013). Kocamemi and Cecen (2005)

480   found that ammonium and TCE compete for the same active sites of the enzyme ammonia

481   monooxygenase. In a mixed culture study containing *Nitrosomonas europaea,* Kocamemi and Cecen

482   (2010) found that the transformation yield for TCE was strongly dependent on initial ammonium and

483   TCE concentrations, with a minimum initial level of 3 μM of ammonium required to transform the

484   maximum initial TCE concentration of 7 μM. We are not aware of any studies which have considered

485   hyporheic nitrification as a natural attenuation process for CEs under field conditions.

486   ### 2.4.5   Interaction between aerobic and anaerobic VC transformation pathways

487   Ethene-assimilating bacteria (ethenotrophs) can oxidise ethene as the sole carbon and energy

488   source and simultaneously transform VC co-metabolically whereas VC-assimilating bacteria can use

489   VC as the sole carbon and energy source (Mattes et al., 2010). Therefore, when anoxic groundwater

490   containing VC and ethene migrates through the mixing zones around HFCs, there is a potential for

491   assimilation of both substrates by ethenotrophs and VC-assimilators and also co-metabolic VC

492   degradation by ethenotrophs growing on ethene (Atashgahi et al., 2017a). Such synergetic interactions

493   can be further enhanced by methanotrophs that can oxidize both ethene and VC. In line with this, a

494   recent study using groundwater microcosms showed that when methane, ethene and VC were added to

495   microcosms, the rate of VC removal was faster than with either methane or ethene alone, consistent with

496   the idea that methanotrophs stimulate ethenotrophic removal of VC (Findlay et al., 2016). Moreover,

497   recent studies have shown that reductive dechlorination can impact aerobic VC degradation pathways

498   in hyporheic zones. Microcosms prepared from fine-grained, SOM-rich sediments with high reductive

499   dechlorination capacity did not have the potential for metabolic aerobic VC oxidation (Atashgahi et al.,

500   2013, 2017a). Under atmospheric O_2 conditions, *D. mccartyi* was protected from O_2 toxicity by the

501   sediment structure and grew by reductive dechlorination of VC. No ethene accumulation was noted

502   indicating the activity of ethenotrophs (Atashgahi et al., 2013, 2017a) which can, in turn, co-

503 metabolically oxidise VC (Findlay et al., 2016). In contrast, metabolic aerobic VC activity was observed

504 from microcosms prepared from sediments with low SOM, coarse grain size and low reductive

505 dechlorination potential. The study showed that local sediment geochemistry and reductive

506 dechlorination highly impact metabolic versus co-metabolic aerobic VC degradation pathway. Where

507 low reductive potential was noted, ethenotrophs exposed to continuous VC flow in oxic sediment layers

508 might adapt to metabolic aerobic VC degradation (Atashgahi et al., 2017a). These findings are consistent

509 with upon extended exposure to VC, ethenotrophic strains of *Mycobacterium* (Jin and Mattes, 2008) and

510 *Pseudomonas* (Verce et al., 2001) transit from co-metabolic to growth-linked VC mineralisation.

511 **3   Field-scale conceptualisation challenges and potential solutions**

512 **3.1   Spatial variability of potential transformation zones**

513   **3.1.1   OHRB occurrence in riverbed sediments**

514   qPCR approaches targeting 16S rRNA genes and reductive dehalogenation catabolic genes (*rdhA*)

515 (Lu et al., 2015) have been used to track the presence and activity of OHRB in hyporheic zones

516 (Vandermeeren et al., 2014). These biomarkers have revealed a close association with OHRB, SOM

517 content and grain-size distribution in organohalide-impacted hyporheic sediments (Atashgahi et al.,

518 2013; Kranzioch et al., 2013; Hamonts et al., 2014; Atashgahi et al., 2015). In a survey of OHRB in

519 relation to hexachlorobenzene (HCB) fate in 15 riverbed sediment locations across four European

520 catchments, Taş et al., (2011) detected *D. mccartyi* 16S rRNA genes at 80% of sites though their counts

521 did not surpass 0.1% of total bacterial 16S rRNA gene copies. HCB half-lives ranged from a few days

522 to up to one month. A relatively weak correlation was observed between decay rate and number of *D.*

523 *mccartyi* suggesting additional OHR activity from other OHRB. Atashgahi et al. (2013) used 16S rRNA

524 of *D. mccartyi* and genes encoding for VC reductive dehalogenase enzymes (*vcrA* and *bvcA*) to track

525 dominant VC biotransformation processes in microcosms prepared from hyporheic sediments. *D.*

526 *mccartyi* had a dominant role on VC removal in microcosms prepared from coarse-grained bed

527 sediments with an abundance of SOM. A subsequent in situ study at the same site showed a reduced VC

528 respiration potential due to construction of a wastewater treatment plant upstream of the study area that

529 resulted in a reduction of organic matter loading to the riverbed sediments (Atashgahi et al., 2015).

530 Similarly, PCR detection of *D. mccartyi* was reported to be closely linked with SOM content and

531 sediment particle size (Abe et al., 2009). This work showed that *D. mccartyi* presence in the sediment

532 profile was spatially correlated with SOM where it exceeded 2% (g/g) with stronger signals occurring

533 at greater depth. A recent study by Simsir et al. (2017) investigated CEs discharging to a creek in

534 Tennessee from organohalide-contaminated fractured bedrock (Table 1). Over a 300 m river section,

535 16S rRNA genes of *D. mccartyi* and *Dehalobacter* were found to be more abundant in deeper sediment

536 layers (50 cm) coincident with higher concentrations of cDCE and VC. Their study revealed the presence

537 of multiple strains of *D. mccartyi* occurring together and expressing functional genes involved in

538 respiration of CE (e.g. *tceA*, *bvcA* and *vcrA)* and chlorinated ethane/methane (*dcpA*).

539 ### 3.1.2 Plume-scale discharge and transformation controls

540 Groundwater plume discharge and transformation patterns are controlled by the spatial

541 distribution and continuity of sediment domains with distinct hydraulic properties along river corridors

542 (Fleckenstein et al., 2006; Wondzell, 2011). The available field investigations (Table 1) have shown that

543 low-K sediments (e.g. clay and silt) are the most important local controls on contaminant discharge in

544 heterogeneous sediment sequences. For example, at the Pine River PCE plume site in Ontario (Conant

545 et al., 2004; Abe et al., 2009) and for a TCE plume discharging to the River Tern in the UK (Weatherill

546 et al., 2014), the lateral and longitudinal continuity of semi-confining silty deposits were shown to

547 control the location and magnitude of plume discharge (Table 1, Fig. 6). Where these low-K sediments

548 also contain SOM, conditions for enhanced biotransformation may also occur where residence times are

549 greatly extended due to hydrophobic portioning to the organic carbon present. This is demonstrated by

550 Conant et al. (2004) and Abe et al. (2008) for the Pine River site with extensive in-situ transformation

551 of PCE or TCE to cDCE (Fig. 6) reported. The importance of low-K layers in contaminant

552 transformation has been illustrated in a modelling study by Gomez-Velez et al. (2014). Their work has

553 shown that the interfaces of sediments with large K contrasts can sequester upwelling groundwater by

554 creating stagnation zones which facilitate mixing of waters with different residence times. Hyporheic

555 exchange patterns arising from riverbed topography have also been shown to influence patterns of in-

556 situ transformation of discharging groundwater plumes. With the benefit of chloride as a conservative

557 surface water tracer, Freitas et al. (2015) observed TCE transformation associated with coarse grained

558   sediment along a riffle sequence of the River Tame (Birmingham, UK) where river water infiltration

559   carrying DOC was inferred from chloride profiles. In one location (Fig. 6) up to 80% TCE conversion

560   to ethene was reported. In-situ dechlorination was also shown to be largely absent along the investigation

561   corridor where riverbed topography was subdued.

562   The presence of preferential pathways with short residence times (such as springs) afford little

563   opportunity for in-situ natural attenuation (e.g. Fryar et al., 2000; LaSage et al., 2008; Rønde et al.,

564   2017). This mode of contaminant discharge arises where discontinuities occur in low-permeability

565   alluvial architecture that act as high-flux 'geological windows' (Conant et al., 2004; Weatherill et al.,

566   2014). For example, through temperature mapping, Conant (2004) found that nearly a quarter of the

567   baseflow accretion along a reach of the Pine River in Angus occurred from just 7% of the riverbed area.

568   The available case studies (Table 1) highlight the patchy nature of natural attenuation zones where the

569   mass fluxes to surface water are dominated by small areas through which most groundwater baseflow

570   discharge is concentrated.

571   **3.1.3   Pore-scale mass transport and processing**

572   Microbial metabolic activity and diversity in riverbeds has been reported to be concentrated in

573   the uppermost 50–60 cm of hyporheic sediment sequences (Franken et al., 2001; Freixia et al., 2016).

574   Heterotrophic microbes (including OHRB) are predominantly found attached to sediment surfaces in

575   epilithic biofilms (Davey and O'Toole, 2000). Hyporheic biofilms comprise diverse assemblages of

576   fungi, algae and microbial consortia enveloped by a matrix of extracellular polymeric substances (EPS)

577   through which diffusive transport of solutes predominates (Storey et al., 1999; Battin et al., 2016).

578   Biofilm structures have been shown to retain and process complex DOM in sediments (Fischer et al.,

579   2005; Bengtsson et al., 2014) and may be important sites of SCFA fermentation (Rulík and Hereka,

580   1998; Rulík et al., 2000). Biofilm accumulation in interstitial spaces is known to decrease the bulk K

581   and effective porosity of sediments in downwelling zones, thereby reducing hydrodynamic exchange

582   with the overlying water column (Battin et al., 1997; 2003; 2008; Mermillod-Blondin et al., 2005) and

583   inducing redox gradients (Boano et al., 2014). Biofilm development may be facilitated in downwelling

584   streambed zones during the clogging of coarse sediment pore spaces (colmation) by non-settlable POM

585   originating from surface water sources (Navel et al., 2012).

586   The convolution of flow paths through heterogeneous biofilm-enveloped sediments produces a

587   scale dependence in chemical reaction rates where microbial processes are superimposed on larger-scale

588   advective solute fluxes that deliver reactants (Sobczak and Findlay, 2002; Findlay et al., 2003; Nogaro

589   et al., 2013). Mendoza-Lera et al. (2017) propose a conceptual framework unifying hyporheic flow and

590   biogeochemical transformation capacity in riverbeds which is applicable for both anaerobic and aerobic

591   biotransformation of CEs. They propose that biogeochemical processing is controlled by the mass

592   transfer of key reactants (TEAs, fermentable DOM and nutrients) and the sediment surface area

593   available for biofilm colonisation. Mass transfer is characterised in three stages, the slowest of which

594   will be the rate-limiting step for biotransformation: (1) transfer from bulk groundwater or surface water

595   to the hyporheic environment (2) transfer from sediment pore water into microbial biofilms and (3)

596   membrane transfer from the extracellular biofilm matrix into individual cells. The sediment particle size

597   controls the surface area for colonisation which is inversely proportional to K. High K sediments (such

598   as gravel bars) exhibit high mass transfer rates but low processing capacities. Conversely, low K

599   sediments (e.g. silts and clays) have very high areas for colonisation due to the huge surface area to

600   sediment volume ratio present but mass transport is slow and diffusion-limited. Their model assumes

601   that solute uptake rates follow Michaelis-Menten kinetics where microbial activity increases

602   proportionally with the mass transfer rate until a saturation point is reached (Ribot et al., 2013). This

603   framework supports field observations where enhanced dechlorination activity and OHRB are reported

604   in sediment domains where diffusive transport is locally dominant (Conant et al., 2004; Abe et al., 2009;

605   Damgaard et al., 2013; Atashgahi et al., 2015; 2017a). Biofilm colonisation is also influenced by changes

606   in pore water temperature, pH and light exposure as well as sediment surface roughness (Gette-Bouvarot

607   et al., 2015; Voisin et al., 2016).

608   Delivery of CEs into reactive diffusion-dominated pore water systems will be dependent on the

609   presence, connectivity and residence time of macropore flow paths which facilitates advective transfer

610   from bulk upwelling groundwater (e.g. Bohlke et al., 2007; Chambon et al., 2010; Menichino and Hester,

611   2015). Heterogeneity in grain size distribution, particle packing and sphericity can induce locally anoxic

612 or hypoxic microzones where mass transfer rates from bulk water to biofilms vary at the scale of

613 sediment pores (Briggs et al., 2013; 2014). Anoxic microzones have been widely implicated where

614 mixed TEAPs and fermentation reactions appear to occur simultaneously (e.g. Storey et al., 1999; Baker

615 et al., 2000; Mermillod-Blondin et al., 2005) and may explain observed co-activity of aerobes and

616 anaerobes (e.g. Atashgahi et al., 2017a). Using two-dimensional dual-domain pore network models of

617 advective-diffusive transport, Briggs et al. (2015) showed that pore-scale heterogeneity (variation in

618 pore throat size) leads to zones of increased and decreased solute mobility in hyporheic in hyporheic

619 sediments. In the less mobile domain (which is responsible for observed tracer breakthrough tailing),

620 anoxia develops where O_2 consumption exceeds the re-supply rate. These microzones may be

621 cumulatively important in determining the overall transformation capacity of hyporheic sediments. For

622 example, LCEs produced anaerobically in the low-mobility domain are mineralised in the more mobile

623 aerobic domain. This is particularly important in the case of VC which can require only trace oxygen

624 levels to sustain aerobic uptake (Gossett, 2010; Fullerton et al., 2014).

625 **3.2 Multi-scale in-situ characterisation technologies**

626 **3.2.1 Evaluating hydrological connectivity**

627 The natural flow regime heterogeneity of most plume discharge zones makes the design and

628 implementation of effective in-situ monitoring programs non-trivial (Kalbus et al., 2006; Rivett et al.,

629 2008b; Roy and Bickerton, 2010; Burk and Cook, 2015). Heterogeneous sediment sequences present a

630 common challenge for the development of conceptual models of plume fate (Ellis and Rivett, 2007).

631 Direct sediment core sampling can provide intact samples in cohesive sequences but is impractical where

632 granular deposits occur. Freeze-coring methods have been applied to characterise fluvial sediment

633 sequences with mixed grain size distributions (Freitas et al., 2015). However, this extractive technique

634 necessitates disruption of sediment microstructure and associated transport pathways (Descloux et al.,

635 2010). Non-invasive hydrogeophysical 'imaging' technologies have emerged which offer promising

636 insights into the in-situ spatial variability of mass transport pathways at <1 m to >10 m scales. For

637 example, Mermillod-Blondin et al. (2014) used ground-penetrating radar (GPR) to map biologically

638 active domains within a gravel bar sequence of the River Rhone in France. Electrical resistivity imaging

639 technology has been used to image flow-controlling sedimentary structures and electrically conductive

640 solute plume migration at reach-scale (Nyquist et al., 2008; González-Pinzón et al., 2015). Recently,

641 Briggs et al. (2014) applied geoelectrical hysteresis techniques to characterise pore-scale rate-limiting

642 mass transport through dual domain porous media (mobile and less mobile porosity fractions).

643 Temperature mapping using contact probes or continuous optical fibres and has been used to

644 evaluate patchy sub-metre scale connectivity between groundwater and surface water in plan-view when

645 a seasonal thermal gradient is present (Conant, 2004; Tristram et al., 2014; Rosenberry et al., 2016).

646 Groundwater baseflow fluxes through riverbeds have been modelled using one dimensional advective-

647 diffusive heat flow as a surrogate for Darcian flow in grids of riverbed temperature profiles (Schmidt et

648 al., 2006; 2007) where upwelling flow predominates. Both upwelling and downwelling fluxes have more

649 recently been obtained from vertical profiles of riverbed temperature time series (e.g. Anibas et al.,

650 2011; 2016; Munz et al., 2016). Heat pulse injections have been used to understand three-dimensional

651 water fluxes through shallow sandy hyporheic sediments at centimetre scales (Angermann et al., 2012).

652 Recently, point-velocity probing (PVP) has been used to map hydrological connectivity with a

653 comparable resolution to temperature mapping (Rønde et al., 2017). Overall, hydrological connectivity

654 will be highly site-specific and the most useful results will be obtained where multiple techniques are

655 employed with overlapping nested scales (e.g. Milosevic et al., 2012).

656 **3.2.2   Resolving in-situ biogeochemical gradients**

657 Delineation of in-situ vertical chemical gradients has been accomplished using depth-discrete

658 profiling in riverbeds (Fig. 6) over vertical length scales of 0.1 to 3 m (Conant et al., 2004; Rivett et al.,

659 2008b; Krause et al., 2013; Heppel et al., 2014). Multi-port monitoring wells have achieved finer vertical

660 sampling resolution (<0.1 m) in contaminated aquifers (e.g. Jobelius et al., 2011). However, technical

661 challenges and cost implications are often likely to prohibit monitoring installations in riverbeds which

662 require a drilling rig. Instead, hand-portable lightweight installations utilising drive-point and direct-

663 push methods usually offer the most cost-effective solutions (Rivett et al., 2008b; Roy and Bickerton,

664 2010). CE fate in hyporheic systems has been investigated using the 'waterloo profiler' (Pitkin, et al.,

665 1999; Conant et al., 2004) and other pore water samplers (e.g. Hamonts et al., 2012), multi-level sampler

666 bundles (Conant et al., 2004), nested piezometers (Lorah and Olsen, 1999) and drive-point mini-

667   piezometers (Conant et al., 2004; Ellis and Rivett, 2007; Roche et al., 2008). Rivett et al. (2008b) and

668   Typical drive-point methods utilise a temporary casing to protect screens and sampling inlets during

669   installation. Collapse of adjacent sediments is relied upon to provide sufficient sealing action to prevent

670   any preferential flow along this 'short-circuit' pathway. This limitation is overcome with direct-push

671   methods such as that described by Roy and Bickerton (2010). They developed a miniaturised waterloo

672   profiler optimised for rapid acquisition of riverbed sediment pore water using a portable hammer drill.

673   From Fig. 6 and Table 1, it can be seen that the selection of appropriate vertical monitoring scales is

674   site-specific and must be informed by an initial conceptual understanding larger scale water fluxes.

675   Recent field experience suggests vertical resolutions of 0.1 – 0.2 m may be sufficient to capture bulk

676   gradients in pore water chemistry (Fig. 6).

677   A potential monitoring gap exists at µm–mm scales below the sediment-water interface where

678   preservation of natural stratification in pore water chemistry is impossible with extractive sampling

679   techniques. Transformation boundary zones at thin fine-grained sediment strata and critical mixing

680   zones may be overlooked by sampling at coarser resolutions (Hester et al., 2017). In-situ passive

681   sampling technology utilising diffusive pore water equilibration offers a possible means to address this

682   scale gap. Dialysis 'peepers' can provide high-resolution solute profiles using a chambered sampler

683   design (Lewandowski et al., 2002; Tan et al., 2005) and have been used to investigate CE plume fate at

684   centimetre-scale (Lorah and Olsen, 1999; LaSage et al., 2008). Peepers require up to several weeks for

685   concentration equilibration to be achieved between ambient pore water and dialysis cell water during

686   which the sampler is vulnerable to disturbance and transient effects (Tan et al., 2005). Simsir et al.

687   (2017) used direct push diffusion samplers (Fig. 6) comprised of glass vials with polyethene or non-

688   woven porous fabric deployed into shallow creek sediment in Tennessee which were equilibrated for

689   two weeks. Passive sampling technology using hydrogel media requires much shorter equilibration

690   times (24-72 hours) and offers a promising way forward to address the mm monitoring scale gap.

691   Diffusive equilibration or gradient sampling in thin films (DET/DGT) has provided mm-scale depth

692   profiles of inorganic nitrogen species, phosphorus and metals in stream sediments (Davison et al., 1994;

693   Palmer-Felgate et al., 2010; Ullah et al., 2012). This technology has recently been applied to studies of

694   enhanced attenuation of groundwater nitrate in riverbeds influenced by in-stream vegetation growth

695   (Ullah et al., 2014). As Briggs et al. (2015) duly point out, extractive sampling procedures tend to always

696   bias the mobile porosity domain of reactive sediment zones which is overcome by diffusive thin film

697   approaches. This technology offers the best opportunity to capture vertical scales approaching the size

698   of pore networks where key reactive transport features such as anoxic microzones may be resolved. As

699   such, this technology can provide a nested observational capability when combined with larger scale

700   solute profiles for a more integrated understanding of plume behaviour.

701   Given that microbial biomass occurs predominantly as biofilms, microbial sampling in the

702   hyporheic zone is sensitive to particle size distribution given that the surface area available for

703   colonisation decreases with increasing particle size (Mendoza-Lera et al., 2017). Direct sampling of fine

704   sediment fractions for molecular analyses of microbial composition have been taken from surficial

705   sediment layers using piston corers (Atashgahi et al., 2012; Hamonts et al., 2014; Vandermeeren et al.,

706   2014) as well as high resolution sub-sampling of deeper cores (Abe et al., 2009; Atashgahi et al., 2014).

707   These methods are well suited to homogenous silt and clay sediments but are subject to the same

708   limitations for coring in granular deposits discussed above. Microbial 'trapping' using an emplaced

709   porous medium for biofilm colonisation is an established approach in aquifer media (Voisin et al., 2016).

710   At the Tennessee creek, Simsir et al. (2017) were able to measure in-situ changes in microbial

711   community structure at high spatial resolution using Bio-Sep bead traps (www.microbe.com) arranged

712   along a 55 cm vertical profile. By combining microbial and pore water sampling (Fig. 6), their work

713   permitted a comprehensive picture of microbial community structure and biogeochemical gradients to

714   be formed. This approach can offer unique insights on linkages between chemical and microbial factors

715   which govern in-situ biotransformation capacity and is suitable for deployment at a range of scales.

716   **4   Conclusions and outlook**

717   **4.1   Conclusions**

718   Our review has established the degree to which hyporheic zones can serve as natural bioreactors

719   capable of reducing mass fluxes of CEs to surface water from groundwater sources. Although OHRB

720   appear to be relatively widespread in riverbeds, field experience to date has shown that in-situ anoxic

721 biotransformation tends to be patchy (Table 1) where fine-grained or SOM-rich sediments occur (Fig

722 1). Observed transformation extents range from partial TCE to cDCE dechlorination to near-complete

723 stoichiometric conversion of TCE to ethene (Fig. 6). In DOM-dominated foodwebs, OHR requires

724 residence times along discharging groundwater flow paths to exceed the reaction timescales for higher-

725 energy TEAs such as O_2 and nitrate. Here, extracellular H_2 will be closely regulated by interspecies

726 transfers between fermenters and heterotrophs (Fig. 3) such as OHRB and methanogens. Competitive

727 interactions between dechlorinators and mineral reducing TEAPs (particularly sulfate) may inhibit OHR

728 steps, particularly cDCE to VC and VC to ethene (Fig. 4). When H_2 is limiting, OHR may compete with

729 these TEAPs for reducing power. Toxic metabolite formation (e.g. sulfide) may cause inhibition when

730 H_2 is unlimited. Conversely, syntrophic partnerships may develop between OHRB and other

731 hydrogenotrophs which may enhance in-situ biotransformation.

732 Thin mixing zones developing between discharging groundwater and downwelling surface water

733 carrying O_2 may create a dynamic anoxic-oxic interface potentially supporting ethenotrophs,

734 methanotrophs and ammonia oxidisers (Fig. 5). Here, a secondary niche environment for VC

735 mineralisation and to some extent, cDCE via direct metabolism and co-metabolism (from the action of

736 mono-oxygenase enzymes) can complete a coupled anoxic-oxic natural 'treatment' process. The oxic

737 potential of CE attenuation in hyporheic zones has only in the last few years become appreciated but is

738 not widely demonstrated at field scale. The efficacy of this step in the process will be dependent on the

739 presence of suitable aerobes and the thickness of mixing zones relative to discharging groundwater flow

740 paths transporting LCEs and co-substrates such as methane and ammonium produced from DOM

741 metabolism.

742 For both anoxic and oxic zone processes, mass transformation will be controlled by the sediment

743 surface area available for biofilm colonisation, delivery rates of critical reactants (e.g. H_2 or O_2), their

744 reaction timescales and exposure time in reactive zones. Diffusion-limited mass transfer from bulk pore

745 water to biofilm domains is likely to be the most important rate-limiting step governing in-situ

746 biotransformation efficacies. At pore scales, heterogeneity in pore throat size can induce dual mobility

747 porosity domains. Solute exposure timeframes are increased in the less mobile domain where anoxic

748   microsite formation may play an important role in the cumulative impact of processes.

749   Effective in-situ monitoring of hyporheic processes in plume discharge zones necessitates a

750   detailed conceptual understanding of the spatial and temporal variability of water flows and residence

751   times. This is best accomplished using non-invasive hydrogeophysical technologies and the application

752   of heat as a surrogate for advection where overlapping spatial scales may be observed simultaneously.

753   Bulk chemical gradients may be delineated using multi-level profiles with vertical resolutions of 0.1–

754   0.2 m often proving sufficient. Nested monitoring is warranted at critical boundary zones where the

755   local properties of pore networks may exert important cumulative controls on observed

756   biotransformation capacities. Simultaneous microbial and pore water sampling can demonstrate that

757   niche conditions for biotransformation are occurring in-situ and is advocated further.

758   **4.2   Future research opportunities**

759   Additional field experience is required to better address spatial and temporal biotransformation

760   variability and allow predictive models to be developed. Directions to improve the current conceptual

761   understanding are outlined as follows:

762   • Integrated field studies addressing coupled flow and reactive transport along pathways at

763   multiple scales are needed (Oldham et al., 2013; Pinay et al., 2015; Abbot et al., 2016). New in-

764   situ tools have emerged which can quantify residence times at high spatial resolution (e.g. Rønde

765   et al., 2017). Dual reactive-conservative 'smart' tracer studies such as acetate-bromide (Rinehart

766   et al., 2015), acetate-resazurin-resorufin (Briggs et al., 2013) which can quantify both residence

767   time and reaction timescales for TEA-DOC couples offer an integrated way forward.

768   • Capturing in-situ spatial and temporal dynamics of O_2/H_2 gradients along discharging

769   groundwater flow paths. These key end-members alone can provide the critical diagnostic

770   information on redox status and indications of key tipping points and priming events which

771   govern in-situ anaerobic-aerobic biotransformation efficacies.

772   • Finally, these recent advances should be coupled with microbiological studies to better

773   understand the ecophysiology of anaerobic and aerobic CE-transforming microbes and their

774   interaction with biotic and abiotic factors. Overall, interdisciplinary efforts are necessary to

775   enhance understanding of hydrological, chemical, physical and microbial interactions and

776   critical gradients that influence the fate of CE in hyporheic zones.

785   **5   References**

786   Abbott, B.W., Baranov, V., Mendoza-Lera, C., Nikolakopoulou, M., Harjung, A., Kolbe, T.,

787   Balasubramanian, M.N., Vaessen, T.N., Ciocca, F., Campeau, A., Wallin, M.B., 2016. Using multi-

788   tracer inference to move beyond single-catchment ecohydrology. Earth-Sci. Rev. 160, 19–42.

789   Abe, Y., Aravena, R., Zopfi, J., Parker, B., Hunkeler, D., 2009. Evaluating the fate of chlorinated ethenes

790   in streambed sediments by combining stable isotope, geochemical and microbial methods. J. Contam.

791   Hydrol. 107 (1) 10–21.

792   Allen-King, R.M., Grathwohl, P., Ball, W.P., 2002. New modeling paradigms for the sorption of

793   hydrophobic organic chemicals to heterogeneous carbonaceous matter in soils, sediments, and rocks.

794   Adv. Water Resour. 25 (8) 985−1016.

795   Angermann, L., Krause, S., Lewandowski, J., 2012. Application of heat pulse injections for investigating

796   shallow hyporheic flow in a lowland river. Water Resour. Res. 48 (12) W00P02.

797   Anibas, C., Buis, K., Verhoeven, R., Meire, P., Batelaan, O., 2011. A simple thermal mapping method

798   for seasonal spatial patterns of groundwater–surface water interaction. J. Hydrol. 397 (1) 93–104.

799   Anibas, C., Schneidewind, U., Vandersteen, G., Joris, I., Seuntjens, P., Batelaan, O., 2016. From

800   streambed temperature measurements to spatial-temporal flux quantification: Using the LPML method

801   to study groundwater-surface water interaction. Hydrol. Process. 30 203–216.

802   Arciero, D., Vannelli, T., Logan, M., Hopper, A.B., 1989. Degradation of trichloroethylene by the

803   ammonia-oxidizing bacterium *Nitrosomonas europaea*. Biochem. Biophys. Res. Commun. 159 (2) 640–

804   643.

805   Arp, D.J., 1995. Understanding the diversity of trichloroethene co-oxidations. Curr. Opin. Biotechnol.

806   6 (3) 352–358.

807   Atashgahi, S., Aydin, R., Dimitrov, M.R., Sipkema, D., Hamonts, K., Lahti, L., Maphosa, F., Kruse, T.,

808   Saccenti, E., Springael, D., Dejonghe, W., 2015. Impact of a wastewater treatment plant on microbial

809   community composition and function in a hyporheic zone of a eutrophic river. Sci. Rep. 5: 17284.

810   Atashgahi, S., Lu, Y., Ramiro-Garcia, J., Peng, P., Maphosa, F., Sipkema, D., Dejonghe, W., Smidt, H.,

811   Springael, D., 2017a. Geochemical parameters and reductive dechlorination determine aerobic

812   cometabolic vs aerobic metabolic vinyl chloride biodegradation at oxic/anoxic interface of hyporheic

813   zones. Environ. Sci. Technol. 51 (3) 1626–1634.

814   Atashgahi, S., Lu, Y., Smidt, H., 2016. Overview of known organohalide-respiring

815   bacteria−phylogenetic diversity and environmental distribution. In: Lorenz., A., Löffler, F., (Eds.)

816   Organohalide-Respiring Bacteria. Springer Berlin, Heidelberg, pp. 63−105.

817   Atashgahi, S., Maphosa, F., De Vrieze, J., Haest, P.J., Boon, N., Smidt, H., Springael, D., Dejonghe,

818   W., 2014. Evaluation of solid polymeric organic materials for use in bioreactive sediment capping to

819   stimulate the degradation of chlorinated aliphatic hydrocarbons. Appl. Microbiol. Biotechnol. 98 (5)

820   2255–2266.

821   Atashgahi, S., Maphosa, F., Doğan, E., Smidt, H., Springael, D. and Dejonghe, W., 2013. Small-scale

822   oxygen distribution determines the vinyl chloride biodegradation pathway in surficial sediments of

823   riverbed hyporheic zones. FEMS Microbiol. Ecol. 84 (1) 133−142.

824 Atashgahi. S., Lu, Y., Zheng, Y., Saccenti, E., Suarez-Diez, M., Ramiro Garcia, J., Eisenmann, H.,

825 Elsner, M., Stams, A.J.M., Springael, D., Dejonghe, W., Smidt, H. 2017b. Geochemical and microbial

826 community determinants of reductive dechlorination at a site biostimulated with glycerol. Environ.

827 Microbiol. 19 968–981.

828 Aulenta, F., Beccari, M., Majone, M., Papini, M.P., Tandoi, V., 2008. Competition for H_2 between

829 sulfate reduction and dechlorination in butyrate-fed anaerobic cultures. Process Biochem. 43 (2) 161–

830 168.

831 Aulenta, F., Majone, M., Verbo, P., Tandoi, V., 2002. Complete dechlorination of tetrachloroethene to

832 ethene in presence of methanogenesis and acetogenesis by an anaerobic sediment microcosm.

833 Biodegradation 13 (6) 411−424.

834 Aulenta, F., Pera, A., Rossetti, S., Papini, M.P., Majone, M., 2007. Relevance of side reactions in

835 anaerobic reductive dechlorination microcosms amended with different electron donors. Water Res. 41

836 (1) 27−38.

837 Azizian, M.F., Marshall, I.P., Behrens, S., Spormann, A.M., Semprini, L., 2010. Comparison of lactate,

838 formate, and propionate as hydrogen donors for the reductive dehalogenation of trichloroethene in a

839 continuous-flow column. J. Cont. Hydrol. 113 (1) 77−92.

840 Bagley, D.M., Gossett, J.M., 1990. Tetrachloroethene transformation to trichloroethene and cis-1, 2-

841 dichloroethene by sulfate-reducing enrichment cultures. Appl. Environ. Microbiol. 56 (8) 2511−2516.

842 Baker, M.A., Dahm, C.N., Valett, H.M., 1999. Acetate retention and metabolism in the hyporheic zone

843 of a mountain stream. Limnol. Oceanogr. 44 (6) 1530–1539.

844 Baker, M.A., Valett, H.M., Dahm, C.N., 2000. Organic carbon supply and metabolism in a shallow

845 groundwater ecosystem. Ecol. 81 (11) 3133–3148.

846 Baker, M.A., Vervier, P., 2004. Hydrological variability, organic matter supply and denitrification in

847 the Garonne River ecosystem. Freshwater Biol. 49 (2) 181−190.

848 Ballapragada, B.S., Stensel, H.D., Puhakka, J.A., Ferguson, J.F., 1997. Effect of hydrogen on reductive

849 dechlorination of chlorinated ethenes. Environ. Sci. Technol. 31 (6) 1728−1734.

850   Battin, T.J., 1997. Assessment of fluorescein diacetate hydrolysis as a measure of total esterase activity

851   in natural stream sediment biofilms. Sci. Total Environ. 198 (1) 51–60.

852   Battin, T.J., Besemer, K., Bengtsson, M.M., Romani, A.M., Packmann, A.I., 2016. The ecology and

853   biogeochemistry of stream biofilms. Nat. Rev. Microbiol. 14 (4) 251–263.

854   Battin, T.J., Kaplan, L.A., Findlay, S., Hopkinson, C.S., Marti, E., Packman, A.I., Newbold, J.D.,

855   Sabater, F., 2008. Biophysical controls on organic carbon fluxes in fluvial networks. Nat. Geosci. 1 (2)

856   95–100.

857   Battin, T.J., Kaplan, L.A., Newbold, J.D., Hansen, C.M., 2003. Contributions of microbial biofilms to

858   ecosystem processes in stream mesocosms. Nature 426 (6965) 439–442.

859   Bengtsson, M.M., Wagner, K., Burns, N.R., Herberg, E.R., Wanek, W., Kaplan, L.A., Battin, T.J., 2014.

860   No evidence of aquatic priming effects in hyporheic zone microcosms. Sci. Rep. 4 5187.

861   Benker, E., Davis, G.B., Appleyard, S., Barry, D.A., Power, T.R., 1996. Trichloroethene (TCE)

862   contamination in an unconfined sand aquifer underlying a residential area of Perth, Western Australia.

863   Hydrogeol. J. 4 (1) 20–29.

864   Berggren, D.R., Marshall, I.P., Azizian, M.F., Spormann, A.M., Semprini, L., 2013. Effects of sulfate

865   reduction on the bacterial community and kinetic parameters of a dechlorinating culture under chemostat

866   growth conditions. Environ. Sci. Technol. 47 (4) 1879−1886.

867   Binley, A., Ullah, S., Heathwaite, A.L., Heppell, C., Byrne, P., Lansdown, K., Trimmer, M., Zhang, H.,

868   2013. Revealing the spatial variability of water fluxes at the groundwater-surface water interface. Water

869   Resour. Res. 49 (7) 3978–3992.

870   Boano, F., Harvey, J.W., Marion, A., Packman, A.I., Revelli, R., Ridolfi, L., Wörman, A., 2014.

871   Hyporheic flow and transport processes: Mechanisms, models, and biogeochemical implications. Rev.

872   Geophys. 52 (4) 603–679.

873   Böhlke, J.K., O'Connell, M.E., Prestegaard, K.L., 2007. Ground water stratification and delivery of

874   nitrate to an incised stream under varying flow conditions. J. Environ. Qual. 36 (3) 664–680.

875   Bommer, M., Kunze, C., Fesseler, J., Schubert, T., Diekert, G., Dobbek, H., 2014. Structural basis for

876   organohalide respiration. Science, 346 (6208) 455−458.

877   Boopathy, R., Peters, R., 2001. Enhanced biotransformation of trichloroethylene under mixed electron

878   acceptor conditions. Current Microbiol. 42 (2) 134−138.

879   Boulton, A.J., Findlay, S., Marmonier, P., Stanley, E.H., Valett, H. M., 1998. The functional significance

880   of the hyporheic zone in streams and rivers. Ann. Rev. Ecol. Syst. 29 59–81.

881   Brablcova, L., Buriánková, I., Badurova, P., Chaudhary, P.P., Rulik, M., 2015. Methanogenic archaea

882   diversity in hyporheic sediments of a small lowland stream. Anaerobe. 32 24−31.

883   Bradley, P., Chapelle, F., 1998b. Microbial mineralization of VC and DCE under different terminal

884   electron accepting conditions. Anaerobe, 4 (2) 81–87.

885   Bradley, P.M., Chapelle, F.H., 1998a. Effect of contaminant concentration on aerobic microbial

886   mineralization of DCE and VC in stream-bed sediments. Environ. Sci. Technol. 32 (5) 553−557.

887   Bradley, P.M., Chapelle, F.H., 2000. Aerobic microbial mineralization of dichloroethene as sole carbon

888   substrate. Environ. Sci. Technol. 34 (1) 221−223.

889   Bradley, P.M., Chapelle, F.H., 2011. Microbial mineralization of dichloroethene and vinyl chloride

890   under hypoxic conditions. Groundwater Monit. Remediat. 31 (4) 39–49.

891   Briggs, M.A., Buckley, S.F., Bagtzoglou, A.C., Werkema, D.D., Lane, J.W., 2016. Actively heated

892   high-resolution fiber-optic-distributed temperature sensing to quantify streambed flow dynamics in

893   zones of strong groundwater upwelling. Water Resour. Res. 52 (7) 5179–5194.

894   Briggs, M.A., Day-Lewis, F.D., Ong, J.B., Harvey, J.W., Lane, J.W., 2014. Dual-domain mass-transfer

895   parameters from electrical hysteresis: Theory and analytical approach applied to laboratory, synthetic

896   streambed, and groundwater experiments. Water Resour. Res. 50 (10) 8281–8299.

897   Briggs, M.A., Day-Lewis, F.D., Zarnetske, J.P., Harvey, J.W., 2015. A physical explanation for the

898   development of redox microzones in hyporheic flow. Geophys. Res. Lett. 42 (11) 4402–4410.

899   Briggs, M.A., Lautz, L.K., Hare, D.K., 2014. Residence time control on hot moments of net nitrate

900   production and uptake in the hyporheic zone. Hydrol. Process. 28 (11) 3741–3751.

901   Briggs, M.A., Lautz, L.K., Hare, D.K., González-Pinzón, R., 2013. Relating hyporheic fluxes, residence

902   times, and redox-sensitive biogeochemical processes upstream of beaver dams. Freshwater Sci. 32 (2)

903   622−641.

904   Burk, L., Cook, P.G., 2015. A simple and affordable system for installing shallow drive point

905   piezometers. Groundwater Monit. Remediat. 35 (3) 101–104.

906   Burston, M.W., Nazari, M.M., Bishop, P.K., Lerner, D.N., 1993. Pollution of groundwater in the

907   Coventry region (UK) by chlorinated hydrocarbon solvents. J. Hydrol. 149 (1–4), 137–161.

908   Buss, S., Cai, Z., Cardenas, B., Fleckenstein, J., Hannah, D., Heppell, K., Hulme, P., Ibrahim, T.,

909   Kaeser, D., Krause, S., Lawler, D., Lerner, D., Mant, J., Malcolm, I., Old, G., Parkin, G., Pickup, R.,

910   Pinay, G., Porter, J., Rhodes, G., Richie, A., Riley, J., Robertson, A.L., Sear, D., Shields, B., Smith,

911   J., Tellam, J., Wood, P., 2009. The Hyporheic Handbook: A handbook on the groundwater -

912   surface-water interface and ecology of the hyporheic zone for environmental managers. Environment

913   Agency Science Report SC0 50070. Environment Agency, Bristol, UK.

914   Byrne, P., Binley, A., Heathwaite, A.L., Ullah, S., Heppell, C.M., Lansdown, K., Zhang, H., Trimmer,

915   M., Keenan, P., 2014. Control of river stage on the reactive chemistry of the hyporheic zone. Hydrol.

916   Process. 28 (17) 4766–4779.

917   Caccavo, F., Jr., Blakemore, R.P., Lovley, D.R., 1992. A hydrogen-oxidizing, Fe(III)-reducing

918   microorganism from the Great Bay estuary, New Hampshire. Appl. Environ. Microbiol. 58 3211–3216.

919   Cardenas, M.B., 2009. Stream-aquifer interactions and hyporheic exchange in gaining and losing

920   sinuous streams. Water Resour. Res. 45 (6) W06429.

921   Cardenas, M.B., 2015. Hyporheic zone hydrologic science: A historical account of its emergence and a

922   prospectus. Water Resour. Res. 51 (5) 3601–3616.

923   Cardenas, M.B., Ford, A.E., Kaufman, M.H., Kessler, A.J., Cook, P.L., 2016. Hyporheic flow and

924   dissolved oxygen distribution in fish nests: The effects of open channel velocity, permeability patterns,

925   and groundwater upwelling. J. Geophys. Res. Biogeosci. 121 (12) 3113–3130.

926   Chambon, J.C., Bjerg, P.L., Scheutz, C., Bælum, J., Jakobsen, R., Binning, P.J., 2013. Review of

927   reactive kinetic models describing reductive dechlorination of chlorinated ethenes in soil and

928   groundwater. Biotechnol. Bioeng, 110 (1) 1−23.

929   Chambon, J.C., Broholm, M.M., Binning, P.J. Bjerg, P.L. 2010. Modeling multi-component transport

930   and enhanced anaerobic dechlorination processes in a single fracture-clay matrix system. J. Cont.

931   Hydrol. 112 77−90.

932   Chan, B., Radom, L., 2011. Assessment of theoretical procedures for hydrogen-atom abstraction by

933   chlorine, and related reactions. Theor. Chem. Acc. 130 (2-3) 251−260.

934   Chan, W.W., Grostern, A., Löffler, F.E., Edwards, E.A., 2011. Quantifying the effects of 1,1,1-

935   trichloroethane and 1,1-dichloroethane on chlorinated ethene reductive dehalogenases. Environ. Sci.

936   Technol. 45 (22) 9693−9702.

937   Chapelle, F.H., Bradley, P.M., McMahon, P.B., Kaiser, K., Benner, R., 2012. Dissolved oxygen as an

938   indicator of bioavailable dissolved organic carbon in groundwater. Ground Water 50 (2) 230–241.

939   Chapman, S.W., Parker, B.L., Cherry, J.A., Aravena, R. Hunkeler, D., 2007. Groundwater–surface

940   water interaction and its role on TCE groundwater plume attenuation. J. Contam. Hydrol. 91 (3) 203–

941   232.

942   Chen, I.M., Chang, B.V., Yuan, S.Y., Wang, Y.S., 2002. Reductive dechlorination of

943   hexachlorobenzene under various additions. Water Air Soil Pollut. 139 (1) 61−74.

944   Christof, O., Seifert, R., Michaelis, W., 2002. Volatile halogenated organic compounds in European

945   estuaries. Biogeochemistry, 59 (1) 143–160.

946   Chung, J., Rittmann, B.E., 2008. Simultaneous bio-reduction of trichloroethene, trichloroethane, and

947   chloroform using a hydrogen-based membrane biofilm reactor. Water Sci. Technol. 58 (3) 495−501.

948   Coleman, N.V., Mattes, T.E., Gossett, J.M., Spain, J.C., 2002. Biodegradation of cis-dichloroethene as

949   the sole carbon source by a β-proteobacterium. Appl. Environ. Microbiol. 68 (6) 2726−2730.

950   Conant, B., 2004. Delineating and quantifying ground water discharge zones using streambed

951   temperatures. Ground water, 42 (2) 243–257.

952   Conant, B., Cherry, J.A. Gillham, R.W., 2004. A PCE groundwater plume discharging to a river:

953   influence of the streambed and near-river zone on contaminant distributions. J. Contam. Hydrol. 73 (1)

954   249–279.

955   Conrad, M.E., Brodie, E.L., Radtke, C.W., Bill, M., Delwiche, M.E., Lee, M.H., Swift, D.L., Colwell,

956   F.S., 2010. Field evidence for co-metabolism of trichloroethene stimulated by addition of electron donor

957   to groundwater. Environ. Sci. Technol. 44 (12) 4697–4704.

958   Cord-Ruwisch, R., Seitz, H.-J., Conrad, R., 1988. The capacity of hydrogenotrophic bacteria to compete

959   for traces of hydrogen depends on the redox potential of the terminal electron acceptor. Arch. Microbiol.

960   149 350–357.

961   Cuthbert, M.O., Mackay, R., Durand, V., Aller, M.F., Greswell, R.B., Rivett, M.O., 2010. Impacts of

962   river bed gas on the hydraulic and thermal dynamics of the hyporheic zone. Adv. Water Resour. 33 (11)

963   1347–1358.

964   Danko, A.S., Luo, M., Bagwell, C.E., Brigmon, R.L., Freedman, D.L., 2004. Involvement of linear

965   plasmids in aerobic biodegradation of vinyl chloride. Appl. Environ. Microbiol. 70 (10) 6092−6097.

966   Davey, M.E., O'Toole, G.A., 2000. Microbial biofilms: from ecology to molecular genetics. Microbiol.

967   Mol. Biol. Rev. 64 (4) 847–867.

968   Davison, W., Zhang, H., Grime, G. W., 1994. Performance characteristics of gel probes used for

969   measuring the chemistry of pore waters. Environ. Sci. Technol. 28 1623–1632.

970   Descloux, S., Datry, T., Philippe, M., Marmonier, P., 2010. Comparison of different techniques to assess

971   surface and subsurface streambed colmation with fine sediments. Int. Rev. Hydrobiol. 95 (6) 520–540.

972   Diekert, G., Wohlfarth, G., 1994. Metabolism of homoacetogens. Antonie van Leeuwenhoek, 66 (1)

973   209–221.

974   Dolfing, J., Beurskens, J. E. M., 1995. The microbial logic and environmental significance of reductive

975   dehalogenation. In: Jones, J.G., (Ed.), Advances in microbial ecology 14, Plenum Press, New York, pp

976   143–206.

977   Donn, M.J., Barron, O.V., 2013. Biogeochemical processes in the groundwater discharge zone of urban

978   streams. Biogeochemistry 115 (1-3) 267–286.

979   Duhamel, M., Wehr, S.D., Yu, L., Rizvi, H., Seepersad, D., Dworatzek, S., Cox, E.E., Edwards, E.A.,

980   2002. Comparison of anaerobic dechlorinating enrichment cultures maintained on tetrachloroethene,

981   trichloroethene, cis-dichloroethene and vinyl chloride. Water Res. 36 (17) 4193−4202.

982   Dupont, R.R., Sorensen, D.L., McLean, J.E., Doucette, B.J., Loucks, M., 2003. Enhancement of

983   trichloroethylene degradation via carbon donor and microbial amendment addition. In: Magar, V.S.,

984   Kelley, M.E., (Eds.), Proceedings of the Seventh International In Situ and On-site Bioremediation

985   Symposium, Orlando, Florida, USA, 25 June 2003. Battelle Press, Columbus, OH, p. A-26.

986   Egli, T., 2010. How to live at very low substrate concentration. Water Res. 44 (17) 4826–4837.

987   Elango, V.K., Liggenstoffer, A.S., Fathepure, B.Z., 2006. Biodegradation of vinyl chloride and cis-

988   dichloroethene by a *Ralstonia* sp. strain TRW-1. Appl. Microbiol. Biotechnol. 72 (6) 1270−1275.

989   Ellis, P.A., Rivett, M.O., 2007. Assessing the impact of VOC-contaminated groundwater on surface

990   water at the city scale. J. Contam. Hydrol. 91 (1) 107–127.

991   Fennell, D.E., Gossett, J.M., Zinder, S.H., 1997. Comparison of butyric acid, ethanol, lactic acid, and

992   propionic acid as hydrogen donors for the reductive dechlorination of tetrachloroethene. Environ. Sci.

993   Technol. 31 (3) 918–926.

994   Findlay, M., Smoler, D.F., Fogel, S. Mattes, T.E., 2016. Aerobic vinyl chloride metabolism in

995   groundwater microcosms by methanotrophic and etheneotrophic bacteria. Environ. Sci. Technol. 50 (7)

996   3617–3625.

997 Findlay, S.E., Sinsabaugh, R.L., Sobczak, W.V., Hoostal, M., 2003. Metabolic and structural response

998 of hyporheic microbial communities to variations in supply of dissolved organic matter. Limnol.

999 Oceanogr. 48 (4) 1608–1617.

1000 Fischer, H., Kloep, F., Wilzcek, S., Pusch, M.T., 2005. A river's liver–microbial processes within the

1001 hyporheic zone of a large lowland river. Biogeochemistry 76 (2) 349–371.

1002 Fleckenstein, J.H., Niswonger, R.G., Fogg, G.E., 2006. River-aquifer interactions, geologic

1003 heterogeneity, and low-flow management. Ground water, 44 (6) 837–852.

1004 Forrester, S.B., Han, J.I., Dybas, M.J., Semrau, J.D., Lastoskie, C.M., 2005. Characterization of a mixed

1005 methanotrophic culture capable of chloroethylene degradation. Environ. Eng. Sci. 22 (2) 177–186.

1006 Fox, A., Boano, F., Arnon, S., 2014. Impact of losing and gaining streamflow conditions on hyporheic

1007 exchange fluxes induced by dune-shaped bed forms. Water Resour. Res. 50 (3) 1895−1907.

1008 Franken, R.J., Storey, R.G., Williams, D.D., 2001. Biological, chemical and physical characteristics of

1009 downwelling and upwelling zones in the hyporheic zone of a north-temperate stream. Hydrobiologia,

1010 444 (1-3) 183–195.

1011 Freitas, J.G., Rivett, M.O., Roche, R.S., Durrant, M., Walker, C., Tellam, J.H., 2015. Heterogeneous

1012 hyporheic zone dechlorination of a TCE groundwater plume discharging to an urban river reach. Sci.

1013 Total Environ. 505 236–252.

1014 Freixa, A., Rubol, S., Carles-Brangarí, A., Fernàndez-Garcia, D., Butturini, A., Sanchez-Vila, X.,

1015 Romaní, A.M., 2016. The effects of sediment depth and oxygen concentration on the use of organic

1016 matter: an experimental study using an infiltration sediment tank. Sci. Total Environ. 540 20–31.

1017 Fryar, A.E., Wallin, E.J., Brown, D.L., 2000. Spatial and temporal variability in seepage between a

1018 contaminated aquifer and tributaries to the Ohio River. Groundwater Monit. Remediat. 20 (3) 129–146.

1019 Fullerton, H., Rogers, R., Freedman, D.L., Zinder, S.H., 2014. Isolation of an aerobic vinyl chloride

1020 oxidizer from anaerobic groundwater. Biodegradation 25 (6) 893−901.

1021 Gavala, H.N., Angelidaki, I., Ahring, B.K., 2003. Kinetics and modeling of anaerobic digestion process.

1022 In: Ahring, B.K. (Ed.) Biomethanation I. Springer Berlin Heidelberg, pp. 57–93.

1023 Gette-Bouvarot, M., Mermillod-Blondin, F., Lemoine, D., Delolme, C., Danjean, M., Etienne, L. and

1024 Volatier, L., 2015. The potential control of benthic biofilm growth by macrophytes—A mesocosm

1025 approach. Ecol. Eng. 75 178–186.

1026 Giovannini, G., Donoso-Bravo, A., Jeison, D., Chamy, R., Ruíz-Filippi, G., Wouwer, A.V., 2016. A

1027 review of the role of hydrogen in past and current modelling approaches to anaerobic digestion

1028 processes. Int. J. Hydrogen Energy 41 (39) 17713−17722.

1029 Gomez-Velez, J.D., Krause, S., Wilson, J.L., 2014. Effect of low-permeability layers on spatial patterns

1030 of hyporheic exchange and groundwater upwelling. Water Resour. Res. 50 (6) 5196–5215.

1031 González-Pinzón, R., Ward, A.S., Hatch, C.E., Wlostowski, A.N., Singha, K., Gooseff, M.N., Haggerty,

1032 R., Harvey, J.W., Cirpka, O.A., Brock, J.T., 2015. A field comparison of multiple techniques to quantify

1033 groundwater–surface-water interactions. Freshwater Sci. 34 (1) 139–160.

1034 Gossett, J.M., 2010. Sustained aerobic oxidation of vinyl chloride at low oxygen concentrations.

1035 Environ. Sci. Technol. 44 (4) 1405–1411.

1036 Haest, P.J., Philips, J., Springael, D., Smolders, E., 2011. The reactive transport of trichloroethene is

1037 influenced by residence time and microbial numbers. J. Cont. Hydrol. 119 (1) 89–98.

1038 Haggerty, R., Wondzell, S.M., Johnson, M.A., 2002. Power-law residence time distribution in the

1039 hyporheic zone of a 2nd-order mountain stream. Geophys. Res. Let. 29 (13) 18-1–18-4.

1040 Hallenbeck, P.C., Ghosh, D., 2009. Advances in fermentative biohydrogen production: the way

1041 forward? Trends Biotechnol. 27 (5) 287–297.

1042 Hamonts, K., Kuhn, T., Maesen, M., Bronders, J., Lookman, R., Kalka, H., Diels, L., Meckenstock,

1043 R.U., Springael, D., Dejonghe, W., 2009. Factors determining the attenuation of chlorinated aliphatic

1044 hydrocarbons in eutrophic river sediment impacted by discharging polluted groundwater. Environ. Sci.

1045 Technol. 43 (14) 5270–5275.

1046 Hamonts, K., Ryngaert, A., Maesen, M., Vos, J., Wilzcek, D., Bronders, J., Diels, L., Dejonghe, W.,

1047 Dijk, J., Springael, D., Sturme, M., 2007. Sediment biobarriers for chlorinated aliphatic hydrocarbons

1048 in groundwater reaching surface water (SEDBARCAH Project). In: Hull R.N., Barbu CH., Goncharova

1049 N. (Eds.) Strategies to enhance environmental Security in Transition Countries. NATO Science for

1050 Peace and Security Series C: Environmental Security. Springer, Dordrecht, pp. 249–261.

1051 Hamonts, K., Ryngaert, A., Smidt, H., Springael, D., Dejonghe, W., 2014. Determinants of the microbial

1052 community structure of eutrophic, hyporheic river sediments polluted with chlorinated aliphatic

1053 hydrocarbons. FEMS Microbial. Ecol. 87 (3) 715−732.

1054 Harkness, M., Fisher, A., Lee, M.D., Mack, E.E., Payne, J.A., Dworatzek, S., Roberts, J., Acheson, C.,

1055 Herrmann, R., Possolo, A., 2012. Use of statistical tools to evaluate the reductive dechlorination of high

1056 levels of TCE in microcosm studies. J. Cont. Hydrol. 131 (1) 100−118.

1057 Hartmans, S., De Bont, J.A., 1992. Aerobic vinyl chloride metabolism in *Mycobacterium aurum* L1.

1058 Appl. Environ. Microbiol. 58 (4) 1220−1226.

1059 Hartmans, S., De Bont, J.A.M., Tramper, J., Luyben, K.C.A., 1985. Bacterial degradation of vinyl

1060 chloride. Biotechnol. Let. 7 (6) 383−388.

1061 Harvey, J.W., Bencala, K.E., 1993. The effect of streambed topography on surface-subsurface water

1062 exchange in mountain catchments. Water Resour. Res. 29 (1) 89–98.

1063 He, J., Sung, Y., Dollhopf, M.E., Fathepure, B.Z., Tiedje, J.M., Löffler, F.E., 2002. Acetate versus

1064 hydrogen as direct electron donors to stimulate the microbial reductive dechlorination process at

1065 chloroethene-contaminated sites. Environ. Sci. Technol., 36 (18) 3945−3952.

1066 Heimann, A., Jakobsen, R., Blodau, C., 2009. Energetic constraints on H_2-dependent terminal electron

1067 accepting processes in anoxic environments: a review of observations and model approaches. Environ.

1068 Sci. Technol. 44 (1) 24–33.

1069 Heimann, A.C., Batstone, D.J., Jakobsen, R., 2006. Methanosarcina spp. drive vinyl chloride

1070 dechlorination via interspecies hydrogen transfer. Appl. Environ. Microbiol. 72 (4) 2942−2949.

1071 Helton, A.M., Ardón, M., Bernhardt, E.S., 2015. Thermodynamic constraints on the utility of ecological

1072 stoichiometry for explaining global biogeochemical patterns. Ecol. Lett. 18 (10) 1049–1056.

1073 Heppell, C., Heathwaite, A.L., Binley, A., Byrne, P., Ullah, S., Lansdown, K., Keenan, P., Trimmer,

1074 M., Zhang, H., 2014. Interpreting spatial patterns in redox and coupled water–nitrogen fluxes in the

1075 streambed of a gaining river reach. Biogeochemistry, 117 (2-3) 491−509.

1076 Hester, E.T., Cardenas, M.B., Haggerty, R., Apte, S.V., 2017. The importance and challenge of

1077 hyporheic mixing. Water Resour. Res. DOI: 10.1002/2016WR020005.

1078 Hester, E.T., Young, K.I., Widdowson, M.A., 2013. Mixing of surface and groundwater induced by

1079 riverbed dunes: Implications for hyporheic zone definitions and pollutant reactions. Water Resour. Res.

1080 49 (9) 5221−5237.

1081 Hlaváčová, E., Rulík, M., Čáp, L., 2005. Anaerobic microbial metabolism in hyporheic sediment of a

1082 gravel bar in a small lowland stream. River Res Appl. 21 (9) 1003−1011.

1083 Hoelen, T.P., Cunningham, J.A., Hopkins, G.D., Lebron, C.A., Reinhard, M., 2006. Bioremediation of

1084 cis-DCE at a sulfidogenic site by amendment with propionate. Groundwater Monit. Remediat. 26 (3)

1085 82−91.

1086 Hoelen, T.P., Reinhard, M., 2004. Complete biological dehalogenation of chlorinated ethylenes in

1087 sulfate containing groundwater. Biodegradation 15 (6) 395–403.

1088 Hoelen, T.P., Reinhard, M., 2004. Complete biological dehalogenation of chlorinated ethylenes in

1089 sulfate containing groundwater. Biodegradation 15 (6) 395−403.

1090 Horvath, R.S., 1972. Microbial co-metabolism and the degradation of organic compounds in nature.

1091 Bacteriol. Revs. 36 (2) 146.

1092 Huang, B., Lei, C., Wei, C., Zeng, G., 2014. Chlorinated volatile organic compounds (Cl–VOCs) in

1093 environment–sources, potential human health impacts, and current remediation technologies. Environ.

1094 Int. 71, 118–138.

1095   Hug, L.A., Maphosa, F., Leys, D., Löffler, F.E., Smidt, H., Edwards, E.A., Adrian, L., 2013. Overview

1096   of organohalide-respiring bacteria and a proposal for a classification system for reductive

1097   dehalogenases. Phil. Trans. R. Soc. B 368: 20120322.

1098   Jackson, R.E., 1998. The migration, dissolution, and fate of chlorinated solvents in the urbanized alluvial

1099   valleys of the southwestern USA. Hydrogeol. J. 6 (1), 144–155.

1100   Jahangir, M.M., Khalil, M.I., Johnston, P., Cardenas, L.M., Hatch, D.J., Butler, M., Barrett, M.,

1101   O'flaherty, V., Richards, K.G., 2012. Denitrification potential in subsoils: a mechanism to reduce nitrate

1102   leaching to groundwater. Agric. Ecosyst. Environ. 147 13−23.

1103   Jakobsen, R., Postma, D., 1999. Redox zoning, rates of sulfate reduction and interactions with Fe-

1104   reduction and methanogenesis in a shallow sandy aquifer, Rømø, Denmark. Geochim. Cosmochim.

1105   Acta. 63 (1) 137–151.

1106   Jin, Y. O., Mattes, T. E., 2008. Adaptation of aerobic, ethene assimilating *Mycobacterium* strains to

1107   vinyl chloride as a growth substrate. Environ. Sci. Technol. 42 (13) 4784−4789.

1108   Jobelius, C., Ruth, B., Griebler, C., Meckenstock, R.U., Hollender, J., Reineke, A., Frimmel, F.H.,

1109   Zwiener, C., 2011. Metabolites indicate hot spots of biodegradation and biogeochemical gradients in a

1110   high-resolution monitoring well. Environ. Sci. Technol. 45 (2) 474−481.Jones Jr, J.B., Fisher, S.G.,

1111   Grimm, N.B., 1995. Nitrification in the hyporheic zone of a desert stream ecosystem. J. N. Am. Benthol.

1112   Soc. 14 (2) 249–258.

1113   Jugder, B.E., Ertan, H., Bohl, S., Lee, M., Marquis, C.P., Manefield, M., 2016. Organohalide respiring

1114   bacteria and reductive dehalogenases: key tools in organohalide bioremediation. Front. Microbiol. 7:

1115   249.

1116   Jugder, B.E., Ertan, H., Lee, M., Manefield, M., Marquis, C.P., 2015. Reductive dehalogenases come of

1117   age in biological destruction of organohalides. Trends Biotechnol. 33 (10) 595−610.

1118   Justicia-Leon, S.D., Higgins, S., Mack, E.E., Griffiths, D.R., Tang, S., Edwards, E.A., Löffler, F.E.,

1119   2014. Bioaugmentation with distinct *Dehalobacter* strains achieves chloroform detoxification in

1120   microcosms. Environ. Sci. Technol. 48 (3) 1851−1858.

1121 Kalbus, E., Reinstorf, F., Schirmer, M., 2006. Measuring methods for groundwater-surface water

1122 interactions: a review. Hydrol. Earth Sys. Sci. Discuss. 10 (6) 873–887.

1123 Klier, N.J., West, R.J., Donberg, P.A., 1999. Aerobic biodegradation of dichloroethylenes in surface and

1124 subsurface soils. Chemosphere 38 (5) 1175−1188.

1125 Knapp, J.L., Osenbrück, K., Cirpka, O.A., 2015. Impact of non-idealities in gas-tracer tests on the

1126 estimation of reaeration, respiration, and photosynthesis rates in streams. Water Res. 83 205−216.

1127 Kocamemi, B.A., Çeçen, F., 2005. Cometabolic degradation of TCE in enriched nitrifying batch

1128 systems. J. Hazard. Mater. 125 (1) 260–265.

1129 Kocamemi, B.A., Çeçen, F., 2010. Biological removal of the xenobiotic trichloroethylene (TCE)

1130 through cometabolism in nitrifying systems. Bioresour. Technol. 101 (1) 430–433.

1131 Koch, J. Nowak, W., 2015. Predicting DNAPL mass discharge and contaminated site longevity

1132 probabilities: Conceptual model and high-resolution stochastic simulation. Water Resour. Res. 51 (2)

1133 806–831.

1134 Kranzioch, I., Stoll, C., Holbach, A., Chen, H., Wang, L., Zheng, B., Norra, S., Bi, Y., Schramm, K.W.,

1135 Tiehm, A., 2013. Dechlorination and organohalide-respiring bacteria dynamics in sediment samples of

1136 the Yangtze Three Gorges Reservoir. Environ. Sci. Pollut. Res. 20 (10) 7046−7056.

1137 Krause, S., Hannah, D.M., Fleckenstein, J.H., Heppell, C.M., Kaeser, D., Pickup, R., Pinay, G.,

1138 Robertson, A.L., Wood, P.J., 2011. Inter-disciplinary perspectives on processes in the hyporheic zone.

1139 Ecohydrol. 4 (4) 481–499.

1140 Krause, S., Klaar, M.J., Hannah, D.M., Mant, J., Bridgeman, J., Trimmer, M., Manning-Jones, S., 2014.

1141 The potential of large woody debris to alter biogeochemical processes and ecosystem services in lowland

1142 rivers. Wiley Interdiscip. Rev. Wat. (3) 263–275.

1143 Krause, S., Tecklenburg, C., Munz, M., Naden, E., 2013. Streambed nitrogen cycling beyond the

1144 hyporheic zone: flow controls on horizontal patterns and depth distribution of nitrate and dissolved

1145 oxygen in the upwelling groundwater of a lowland river. J. Geophys. Res. Biogeosci. 118 (1) 54–67.

1146 Krumholz, L.R., Sharp, R., Fishbain, S.S., 1996. A freshwater anaerobe coupling acetate oxidation to
1147 tetrachloroethylene dehalogenation. Appl. Environ. Microbiol. 62 (11) 4108−4113.

1148 Lapworth, D.J., Gooddy, D.C., Allen, D., Old, G.H., 2009. Understanding groundwater, surface water,
1149 and hyporheic zone biogeochemical processes in a Chalk catchment using fluorescence properties of
1150 dissolved and colloidal organic matter. J. Geophys. Res. Biogeosci. 114 G00F02.

1151 LaSage, D.M., Sexton, J.L., Mukherjee, A., Fryar, A.E., Greb, S.F., 2008. Groundwater discharge along
1152 a channelized Coastal Plain stream. J. Hydrol. 360 (1) 252–264.

1153 Laturnus, F., Haselmann, K.F., Borch, T., Grøn, C., 2002. Terrestrial natural sources of trichloromethane
1154 (chloroform, CHCl3)–an overview. Biogeochemistry 60 (2) 121−139.

1155 Lautz, L.K., Fanelli, R.M., 2008. Seasonal biogeochemical hotspots in the streambed around restoration
1156 structures. Biogeochem. 91 (1) 85–104.

1157 Lawrence, J.E., Skold, M.E., Hussain, F.A., Silverman, D.R., Resh, V.H., Sedlak, D.L., Luthy, R.G.,
1158 McCray, J.E., 2013. Hyporheic zone in urban streams: a review and opportunities for enhancing water
1159 quality and improving aquatic habitat by active management. Environ. Eng. Sci. 30 (8) 480–501.

1160 Le, N.B., Coleman, N.V., 2011. Biodegradation of vinyl chloride, cis-dichloroethene and 1, 2-
1161 dichloroethane in the alkene/alkane-oxidising *Mycobacterium* strain NBB4. Biodegradation, 22 (6)
1162 1095–1108.

1163 Lee, I.S., Bae, J.H., McCarty, P.L., 2007. Comparison between acetate and hydrogen as electron donors
1164 and implications for the reductive dehalogenation of PCE and TCE. J. Cont. Hydrol. 94 (1) 76−85.

1165 Lee, M., Low, A., Zemb, O., Koenig, J., Michaelsen, A., Manefield, M., 2012. Complete chloroform
1166 dechlorination by organochlorine respiration and fermentation. Environ. Microbiol. 14 (4) 883−894.

1167 Lewandowski, J., Nützmann, G., 2010. Nutrient retention and release in a floodplain's aquifer and in the
1168 hyporheic zone of a lowland river. Ecol. Eng. 36 (9) 1156–1166.

1169 Lewandowski, J., Rüter, K., Hupfer, M., 2002. Two-dimensional small-scale variability of pore water

1170 phosphate in freshwater lakes: results from a novel dialysis sampler. Environ. Sci. Technol. 36 (9) 2039–

1171 2047.

1172 Leys, D., Adrian, L., Smidt, H., 2013. Organohalide respiration: microbes breathing chlorinated

1173 molecules. Phil. Trans. R. Soc. B 368: 20120316.

1174 Liu, H., Chen, T., Frost, R.L., 2014. An overview of the role of goethite surfaces in the environment.

1175 Chemosphere 103 1−11.

1176 Löffler, F.E., Sanford, R.A., 2005. Analysis of trace hydrogen metabolism. Methods Enzymol. 397 222–

1177 237.

1178 Löffler, F.E., Sun, Q., Li, J., Tiedje, J.M., 2000. 16S rRNA gene-based detection of tetrachloroethene-

1179 dechlorinating *Desulfuromonas* and *Dehalococcoides* species. Appl. Environ. Microbiol. 66 (4)

1180 1369−1374.

1181 Löffler, F.E., Tiedje, J.M., Sanford, R.A., 1999. Fraction of electrons consumed in electron acceptor

1182 reduction and hydrogen thresholds as indicators of halorespiratory physiology. Appl. Environ.

1183 Microbiol. 65 (9) 4049–4056.

1184 Löffler, F.E., Yan, J., Ritalahti, K.M., Adrian, L., Edwards, E.A., Konstantinidis, K.T., Müller, J.A.,

1185 Fullerton, H., Zinder, S.H., Spormann, A.M., 2013. *Dehalococcoides mccartyi* gen. nov., sp. nov.,

1186 obligately organohalide-respiring anaerobic bacteria relevant to halogen cycling and bioremediation,

1187 belong to a novel bacterial class, *Dehalococcoidia* classis nov., order *Dehalococcoidales* ord. nov. and

1188 family *Dehalococcoidaceae* fam. nov., within the phylum *Chloroflexi*. Int. J. Syst. Evol. Microbiol. 63

1189 (2) 625−635.

1190 Lorah, M.M., Dyer, L.J., Burris, D.R., 2007. Anaerobic biodegradation and hydrogeochemical controls

1191 on natural attenuation of trichloroethene in an inland forested wetland. Bioremed. J. 11 (2) 85−102.

1192 Lorah, M.M., Olsen, L.D., 1999. Natural attenuation of chlorinated volatile organic compounds in a

1193 freshwater tidal wetland: Field evidence of anaerobic biodegradation. Water Res. Res. 35 (12) 3811–

1194 3827.

1195 Lovely, D.R., Goodwin, S., 1988. Hydrogen concentrations as an indicator of the predominant

1196 terminal electron accepting process in aquatic sediments. Geochim. Cosmochim. Acta 52 11–18.

1197 Lovley, D. R., 1985, Minimum threshold for hydrogen metabolism in methanogenic bacteria. Appl.

1198 Environ. Microbiol. 49 (6) 1530–1531.

1199 Lovley, D.R., Phillips, E.J.P., Lonergan, D. J., 1989. Hydrogen and formate oxidation coupled to

1200 dissimilatory reduction of iron or manganese by *Alteromonas putrefaciens*. Appl. Environ. Microbiol.

1201 55 700–706.

1202 Lu Y, Atashgahi, S., Hug L.A., Smidt H., 2015. Primers that target functional genes of organohalide-

1203 respiring bacteria. In: McGenity, T.J., Timmis, K.N., Nogales, B., (Eds.) Hydrocarbon and lipid

1204 microbiology protocols: methods to detect specific individuals and groups in communities. Springer

1205 Protocols Handbook. Springer-Verlag, Berlin, Heidelberg. pp. 177–205.

1206 Lu, Q., Luo, Q.S., Li, H., Di Liu, Y., Gu, J.D., Lin, K.F., 2015. Characterization of chlorinated aliphatic

1207 hydrocarbons and environmental variables in a shallow groundwater in Shanghai using kriging

1208 interpolation and multifactorial analysis. PloS one 10 (11), e0142241.

1209 Lu, X.X., Tao, S., Bosma, T., Gerritse, J., 2001. Characteristic hydrogen concentrations for various

1210 redox processes in batch study. J. Environ. Sci. Health Part A, 36 (9) 1725–1734.

1211 Lu, Y., Ramiro-Garcia, J., Vandermeeren, P., Herrmann, S., Cichocka, D., Springael, D., Atashgahi, S.,

1212 Smidt, H., 2017. Dechlorination of three tetrachlorobenzene isomers by contaminated harbor sludge-

1213 derived enrichment cultures follows thermodynamically favorable reactions. Appl. Microbiol. Biotech.

1214 101: 2589–2601.

1215 Luijten, M.L.G.C., Roelofsen, W., Langenhoff, A.A.M., Schraa, G., Stams, A.J. M., 2004. Hydrogen

1216 threshold concentrations in pure cultures of halorespiring bacteria and at a site polluted with chlorinated

1217 ethenes. Environ. Microbiol. 6 (6) 646–650.

1218 Mani, S., Sundaram, J., Das, K.C., 2016. Process simulation and modeling: Anaerobic digestion of

1219 complex organic matter. Biomass and Bioenerg. 93 58−167.

1220   Mao, X., Polasko, A., Alvarez-Cohen, L., 2017. Effects of sulfate reduction on trichloroethene

1221   dechlorination by *dehalococcoides*-containing microbial communities. Appl. Environ. Microbiol. 83 (8)

1222   e03384-16.

1223   Mattes, T.E., Alexander, A.K., Coleman, N.V., 2010. Aerobic biodegradation of the chloroethenes:

1224   pathways, enzymes, ecology, and evolution. FEMS Microbiol. Rev. 34 (4) 445−475.

1225   Mayer-Blackwell, K., Fincker, M., Molenda, O., Callahan, B., Sewell, H., Holmes, S., Edwards, E.A.,

1226   Spormann, A.M., 2016. 1, 2-Dichloroethane exposure alters the population structure, metabolism, and

1227   kinetics of a trichloroethene-dechlorinating *Dehalococcoides mccartyi* consortium. Environ. Sci.

1228   Technol. 50 (22) 12187−12196.

1229   Maymo-Gatell, X., Chien, Y.T., Gossett, J.M., Zinder, S.H., 1997. Isolation of a bacterium that

1230   reductively dechlorinates tetrachloroethene to ethene. Science 276 (5318) 1568−1571.

1231   Maymo-Gatell, X., Nijenhuis, I., Zinder, S.H., 2001. Reductive dechlorination of cis-1,2-dichloroethene

1232   and vinyl chloride by "*Dehalococcoides ethenogenes*". Environ. Sci. Technol. 35 516-−521.

1233   Mazur, C.S., Jones, W.J., 2001. Hydrogen concentrations in sulfate-reducing estuarine sediments during

1234   PCE dehalogenation. Environ. Sci. Technol. 35 4783−4788.

1235   McCarty, P.L., 1997. Breathing with chlorinated solvents. Science 276 (5318) 1521−1522.

1236   McGuire, T.M., Newell, C.J., Looney, B.B., Vangelas, K.M. and Sink, C.H., 2004. Historical analysis

1237   of monitored natural attenuation: A survey of 191 chlorinated solvent sites and 45 solvent plumes.

1238   Remed. J. 15 (1) 99–112.

1239   McKnight, U.S., Funder, S.G., Rasmussen, J.J., Finkel, M., Binning, P.J., Bjerg, P.L., 2010. An

1240   integrated model for assessing the risk of TCE groundwater contamination to human receptors and

1241   surface water ecosystems. Ecol. Eng. 36 1126−1137.

1242   McKnight, U.S., Rasmussen, J.J., Kronvang, B., Bjerg, P.L., Binning, P.J., 2012. Integrated assessment

1243   of the impact of chemical stressors on surface water ecosystems. Sci. Total Environ. 427 319–331.

1244   Meckenstock, R.U., Elsner, M., Griebler, C., Lueders, T., Stumpp, C., Aamand, J., Agathos, S.N.,

1245   Albrechtsen, H.J., Bastiaens, L., Bjerg, P.L., Boon, N., 2015. Biodegradation: updating the concepts of

1246   control for microbial cleanup in contaminated aquifers. Environ. Sci. Technol. 2015, 49, 7073−7081.

1247   Men, Y., Feil, H., VerBerkmoes, N.C., Shah, M.B., Johnson, D.R., Lee, P.K., West, K.A., Zinder, S.H.,

1248   Andersen, G.L., Alvarez-Cohen, L., 2012. Sustainable syntrophic growth of *Dehalococcoides*

1249   *ethenogenes* strain 195 with *Desulfovibrio vulgaris* Hildenborough and *Methanobacterium congolense*:

1250   global transcriptomic and proteomic analyses. ISME J. 6 (2) 410−421.

1251   Men, Y., Lee, P.K., Harding, K.C., Alvarez-Cohen, L., 2013. Characterization of four TCE-

1252   dechlorinating microbial enrichments grown with different cobalamin stress and methanogenic

1253   conditions. Appl. Microbiol. Biotechnol., 97 (14) 6439−6450.

1254   Mendoza-Lera, C., Frossard, A., Knie, M., Federlein, L.L., Gessner, M.O., Mutz, M., 2017. Importance

1255   of advective mass transfer and sediment surface area for streambed microbial communities. Freshwater

1256   Biol. 62 (1) 133–145.

1257   Menichino, G.T., Hester, E.T., 2015. The effect of macropores on bi-directional hydrologic exchange

1258   between a stream channel and riparian groundwater. J. Hydrol. 529 830–842.

1259   Mermillod-Blondin, F., Mauclaire, L., Montuelle, B., 2005. Use of slow filtration columns to assess

1260   oxygen respiration, consumption of dissolved organic carbon, nitrogen transformations, and microbial

1261   parameters in hyporheic sediments. Water Res. 39 (9) 1687–1698.

1262   Mermillod-Blondin, F., Winiarski, T., Foulquier, A., Perrissin, A., Marmonier, P., 2015. Links between

1263   sediment structures and ecological processes in the hyporheic zone: ground-penetrating radar as a

1264   non-invasive tool to detect subsurface biologically active zones. Ecohydrology 8 (4) 626–641.

1265   Meyer, J.L., Paul, M.J., Taulbee, W. K., 2005. Stream ecosystem function in urbanizing landscapes. J.

1266   N. Am. Benthol. Soc. 24, 602−612.

1267   Milosevic, N., Thomsen, N.I., Juhler, R.K., Albrechtsen, H.J., Bjerg, P.L., 2012. Identification of

1268   discharge zones and quantification of contaminant mass discharges into a local stream from a landfill in

1269   a heterogeneous geologic setting. J. Hydrol. 446 13–23.

1270 Mineau, M.M., Rigsby, C.M., Ely, D.T., Fernandez, I.J., Norton, S.A., Ohno, T., Valett, H., Simon,

1271 K.S., 2013. Chronic catchment nitrogen enrichment and stoichiometric constraints on the bioavailability

1272 of dissolved organic matter from leaf leachate. Freshwater Biol. 58 (2) 248–260.

1273 Mohn, W.W., Tiedje, J.M., 1992. Microbial reductive dehalogenation. Microbiol. Rev. 56 (3) 482−507.

1274 Morris, B.E., Henneberger, R., Huber, H., Moissl-Eichinger, C., 2013. Microbial syntrophy: interaction

1275 for the common good. FEMS Microbiol. Rev. 37 (3) 384–406.

1276 Munz, M., Oswald, S.E., Schmidt, C., 2016. Analysis of riverbed temperatures to determine the

1277 geometry of subsurface water flow around in-stream geomorphological structures. J. Hydrol. 539 74–

1278 87.

1279 Naranjo, R.C., Niswonger, R.G., Davis, C.J., 2015. Mixing effects on nitrogen and oxygen

1280 concentrations and the relationship to mean residence time in a hyporheic zone of a riffle-pool sequence.

1281 Water Resour. Res. 51 (9), 7202–7217.

1282 Nath, K., Das, D., 2004. Improvement of fermentative hydrogen production: various approaches. Appl.

1283 Microbiol. Biotechnol. 65 (5) 520–529.

1284 Navel, S., Sauvage, S., Delmotte, S., Gerino, M., Marmonier, P., Mermillod-Blondin, F., 2012. A

1285 modelling approach to quantify the influence of fine sediment deposition on biogeochemical processes

1286 occurring in the hyporheic zone. Ann. Limnol. - Int. J. Lim. 48 279–287.

1287 Nelson, D.K., Hozalski, R.M., Clapp, L.W., Semmens, M.J., Novak, P.J., 2002. Effect of nitrate and

1288 sulfate on dechlorination by a mixed hydrogen-fed culture. Bioremed. J. 6 (3) 225−236.

1289 Ng, D.H., Kumar, A., Cao, B., 2016. Microorganisms meet solid minerals: interactions and

1290 biotechnological applications. Appl. Microbiol. Biotechnol. 100 (16) 6935−6946.

1291 Nogaro, G., Datry, T., Mermillod-Blondin, F., Foulquier, A., Montuelle, B., 2013. Influence of

1292 hyporheic zone characteristics on the structure and activity of microbial assemblages. Freshwater Biol.

1293 58 (12) 2567–2583.

1294 Nogaro, G., Mermillod-Blondin, F., Montuelle, B., Boisson, J.C., Bedell, J.P., Ohannessian, A., Volat,

1295 B., Gibert, J., 2007. Influence of a stormwater sediment deposit on microbial and biogeochemical

1296 processes in infiltration porous media. Sci. Total Environ. 377 (2) 334–348.

1297 Nyquist, J.E., Freyer, P.A., Toran, L., 2008. Stream bottom resistivity tomography to map ground water

1298 discharge. Ground water, 46 (4) 561–569.

1299 Oldenhuis, R., Oedzes, J.Y., Van der Waarde, J.J., Janssen, D.B., 1991. Kinetics of chlorinated

1300 hydrocarbon degradation by Methylosinus trichosporium OB3b and toxicity of trichloroethylene. Appl.

1301 Environ. Microbiol. 57 (1) 7–14.

1302 Oldham, C.E., Farrow, D.E., Peiffer, S., 2013. A generalized Damkohler number for classifying material

1303 processing in hydrological systems. Hydrol. Earth Sys. Sci. Discuss. 17 (3) 1133.

1304 Paes, F., Liu, X., Mattes, T. E., Cupples, A. M., 2015. Elucidating carbon uptake from vinyl chloride

1305 using stable isotope probing and Illumina sequencing. Appl. Microbiol. Biotechnol. 99 (18) 7735−7743.

1306 Palmer-Felgate, E.J., Mortimer, R.J., Krom, M.D., Jarvie, H.P., 2010. Impact of point-source pollution

1307 on phosphorus and nitrogen cycling in stream-bed sediments. Environ. Sci. Technol. 44 (3) 908–914.

1308 Pankow, J.F., Cherry, J.A., 1996. Dense chlorinated solvents and other DNAPLs in groundwater:

1309 History, behavior, and remediation. Waterloo Press, University of Waterloo.

1310 Pantazidou, M., Panagiotakis, I., Mamais, D. and Zikidi, V., 2012. Chloroethene biotransformation in

1311 the presence of different sulfate concentrations. Groundwater Monit. Remediat. 32 (1) 106−119.

1312 Parker, B.L., Gillham, R.W., Cherry, J.A., 1994. Diffusive disappearance of immiscible-phase organic

1313 liquids in fractured geologic media. Ground Water 32 (5) 805–820.

1314 Paul, L., Herrmann, S., Koch, C.B., Philips, J., Smolders, E., 2013. Inhibition of microbial

1315 trichloroethylene dechorination by Fe (III) reduction depends on Fe mineralogy: A batch study using

1316 the bioaugmentation culture KB-1. Water Res. 47 (7) 2543−2554.

1317 Paul, L., Jakobsen, R., Smolders, E., Albrechtsen, H.J., Bjerg, P.L., 2016. Reductive dechlorination of

1318 trichloroethylene (TCE) in competition with Fe and Mn oxides−Observed dynamics in H_2-dependent

1319 terminal electron accepting processes. Geomicrobiol. J. 33 (5) 357−366.

1320 Pavlostathis, S.G., Zhuang, P., 1993. Reductive dechlorination of chloroalkenes in microcosms

1321 developed with a field contaminated soil. Chemosphere 27 (4) 585−595.

1322 Peng, S.B., Huang, J.L., Zhong, X.H., Yang, J.C., Wang, G.H., Zou, Y.B., Zhang, F.S., Zhu, Q.S.,

1323 Buresh, R., Witt, C., 2002. Challenge and opportunity in improving fertilizer-nitrogen use efficiency of

1324 irrigated rice in China. Agr. Sci. China 1 (7) 776−785.

1325 Pérez-de-Mora, A., Zila, A., McMaster, M.L., Edwards, E.A., 2014. Bioremediation of chlorinated

1326 ethenes in fractured bedrock and associated changes in dechlorinating and nondechlorinating microbial

1327 populations. Environ. Sci. Technol. 48 (10) 5770−5779.

1328 Pinay, G., Peiffer, S., De Dreuzy, J.R., Krause, S., Hannah, D.M., Fleckenstein, J.H., Sebilo, M., Bishop,

1329 K., Hubert-Moy, L., 2015. Upscaling nitrogen removal capacity from local hotspots to low stream

1330 orders' drainage basins. Ecosystems 18 (6) 1101–1120.

1331 Pitkin, S.E., Cherry, J.A., Ingelton, R.A., Broholm, M., 1999. Field demonstrations using the Waterloo

1332 groundwater profiler. Ground Water Monit. Remediat. 19 (2) 122–131

1333 Puigserver, D., Cortés, A., Viladevall, M., Nogueras, X., Parker, B.L., Carmona, J.M., 2014. Processes

1334 controlling the fate of chloroethenes emanating from DNAPL aged sources in river–aquifer contexts. J.

1335 Cont. Hydrol. 168 25−40.

1336 Pusch, M., Schwoerbel, J., 1994. Community respiration in hyporheic sediments of a mountain stream

1337 (Steina, Black Forest). Archiv für Hydrobiologie 130 (1) 35−52.

1338 Rahimi, M., Essaid, H.I., Wilson, J.T., 2015. The role of dynamic surface water-groundwater exchange

1339 on streambed denitrification in a first-order, low-relief agricultural watershed. Water Resour. Res. 51

1340 (12) 9514–9538.

1341   Rasche, M.E., Hyman, M.R., Arp, D.J., 1991. Factors limiting aliphatic chlorocarbon degradation by

1342   Nitrosomonas europaea: cometabolic inactivation of ammonia monooxygenase and substrate

1343   specificity. Appl. Environ. Microbiol. 57 (10) 2986–2994.

1344   Rasmussen, J.J., McKnight, U.S., Sonne, A.T., Wiberg-Larsen, P., Bjerg, P.L., 2016. Legacy of a

1345   Chemical Factory Site: Contaminated Groundwater Impacts Stream Macroinvertebrates. Arch. Environ.

1346   Contam. Toxicol. 70 (2) 219–230.

1347   Ribot, M., Von Schiller, D., Peipoch, M., Sabater, F., Grimm, N.B., Martí, E., 2013. Influence of nitrate

1348   and ammonium availability on uptake kinetics of stream biofilms. Freshwater Sci. 32 (4) 1155–1167.

1349   Richardson, R.E., 2016. Organohalide-Respiring Bacteria as Members of Microbial Communities:

1350   Catabolic Food Webs and Biochemical Interactions. In: Lorenz., A., Löffler, F., (Eds.) Organohalide-

1351   Respiring Bacteria. Springer Berlin, Heidelberg, pp. 309−341.

1352   Rinehart, A.J., Jones Jr, J.B., Harms, T.K., 2015. Hydrologic and biogeochemical influences on carbon

1353   processing in the riparian zone of a subarctic stream. Freshwater Sci. 34 (1) 222−232.

1354   Rivett, M.O., Buss, S.R., Morgan, P., Smith, J.W., Bemment, C.D., 2008a. Nitrate attenuation in

1355   groundwater: a review of biogeochemical controlling processes. Water Res. 42 (16) 4215−4232.

1356   Rivett, M.O., Dearden, R.A., Wealthall, G.P., 2014. Architecture, persistence and dissolution of a 20 to

1357   45year old trichloroethene DNAPL source zone. J. Contam. Hydrol. 170, 95–115.

1358   Rivett, M.O., Ellis, P.A., Greswell, R.B., Ward, R.S., Roche, R.S., Cleverly, M.G., Walker, C., Conran,

1359   D., Fitzgerald, P.J., Willcox, T. Dowle, J., 2008b. Cost-effective mini drive-point piezometers and

1360   multilevel samplers for monitoring the hyporheic zone. Q. J. Eng. Geol. Hydr. 41 (1) 49–60.

1361   Rivett, M.O., Feenstra, S., 2005. Dissolution of an emplaced source of DNAPL in a natural aquifer

1362   setting. Environ. Sci. Technol. 39 (2) 447–455.

1363   Rivett, M.O., Feenstra, S., Clark, L., 2006. Lyne and McLachlan (1949): influence of the first

1364   publication on groundwater contamination by trichloroethene. Environ. Forensics 7 (4), 313–323.

1365 Rivett, M.O., Turner, R.J., Glibbery, P., Cuthbert, M.O., 2012. The legacy of chlorinated solvents in the

1366 Birmingham aquifer, UK: Observations spanning three decades and the challenge of future urban

1367 groundwater development. J. Contam. Hydrol. 140, 107–123.

1368 Roche R.S., Rivett M.O., Tellam J.H., Cleverly M.G., Walker M., 2008. Natural attenuation of a TCE

1369 plume at the groundwater–surface-water interface: spatial and temporal variability within a 50 m reach.

1370 GQ07: securing groundwater quality in urban and industrial environments. IAHS Publ., pp. 475–82.

1371 Romaní, A.M., Vázquez, E., Butturini, A., 2006. Microbial availability and size fractionation of

1372 dissolved organic carbon after drought in an intermittent stream: biogeochemical link across the stream–

1373 riparian interface. Microb. Ecol. 52 (3) 501–512.

1374 Rønde, V., McKnight, U.S., Sonne, A.T., Balbarini, N., Devlin, J.F., Bjerg, P.L., 2017. Contaminant

1375 mass discharge to streams: Comparing direct groundwater velocity measurements and multi-level

1376 groundwater sampling with an in-stream approach. J. Cont. Hydrol. DOI:

1377 10.1016/j.jconhyd.2017.09.010

1378 Rosenberry, D.O., Briggs, M.A., Delin, G., Hare, D.K., 2016. Combined use of thermal methods and

1379 seepage meters to efficiently locate, quantify, and monitor focused groundwater discharge to a sand-bed

1380 stream. Water Resour. Res. 52 (6) 4486–4503.

1381 Rowe, B.L., Toccalino, P.L., Moran, M.J., Zogorski, J.S., Price, C.V., 2007. Occurrence and potential

1382 human–health relevance of volatile organic compounds in drinking water from domestic wells in the

1383 United States. Environ. Health Perspect. 115 (11) 1539.

1384 Roy, J.W., Bickerton, G., 2010. Proactive screening approach for detecting groundwater contaminants

1385 along urban streams at the reach-scale. Environ. Sci. Technol. 44 (16) 6088–6094.

1386 Roy, J.W., Bickerton, G., 2011. Toxic groundwater contaminants: an overlooked contributor to urban

1387 stream syndrome? Environ. Sci. Technol.   46 (2) 729–736.

1388 Roy, J.W., Grapentine, L., Bickerton, G., 2017. Ecological effects from groundwater contaminated by

1389 volatile organic compounds on an urban stream's benthic ecosystem. Limnologica–Ecology and

1390 Management of Inland Waters. DOI:10.1016/j.limno.2017.01.004.

1391   Rulík, M., Čáp, L. and Hlaváčová, E., 2000. Methane in the hyporheic zone of a small lowland stream

1392   (Sitka, Czech Republic). Limnologica - Ecology and Management of Inland Waters 30 (4) 359−366.

1393   Rulik, M., Hekera, P., 1998. Occurence of both acetic and lactic acids in subsurface water of the bed

1394   sediments: comparison of two different localities. In: Bretschko, G., Helešivic, J. (Eds.) Advances in

1395   River Bottom Ecology. Backhuys Publishers, Leiden pp. 77−87.

1396   Ryoo, D., Shim, H., Canada, K., Barbieri, P., Wood, T.K., 2000. Aerobic degradation of

1397   tetrachloroethylene by toluene-o-xylene monooxygenase of Pseudomonas stutzeri OX1. Nat.

1398   Biotechnol. 18 (7) 775–778.

1399   Sanders, I.A., Heppell, C.M., Cotton, J.A., Wharton, G., Hildrew, A.G., Flowers, E.J., Trimmer, M.,

1400   2007. Emission of methane from chalk streams has potential implications for agricultural practices.

1401   Freshwater Biol. 52 (6) 1176−1186.

1402   Sawyer, A.H., Cardenas, M.B., 2009. Hyporheic flow and residence time distributions in heterogeneous

1403   cross-bedded sediment. Water Resour. Res. 45 (8) W08406.

1404   Scheutz, C., Durant, N.D., Hansen, M.H., Bjerg, P.L., 2011. Natural and enhanced anaerobic

1405   degradation of 1,1,1-trichloroethane and its degradation products in the subsurface–a critical review.

1406   Water Res. 45 (9) 2701−2723.

1407   Schmidt, C., Bayer-Raich, M., Schirmer, M., 2006. Characterization of spatial heterogeneity of

1408   groundwater-stream water interactions using multiple depth streambed temperature measurements at the

1409   reach scale. Hydrol. Earth Sys. Sci. Discuss. 3 (4) 1419–1446.

1410   Schmidt, C., Conant, B., Bayer-Raich, M., Schirmer, M., 2007. Evaluation and field-scale application

1411   of an analytical method to quantify groundwater discharge using mapped streambed temperatures. J.

1412   Hydrol. 347 (3) 292–307.

1413   Schmidt, K.R., Augenstein, T., Heidinger, M., Ertl, S., Tiehm, A., 2010. Aerobic biodegradation of cis-

1414   1,2-dichloroethene as sole carbon source: stable carbon isotope fractionation and growth characteristics.

1415   Chemosphere, 78 (5) 527−532.

1416 Schmidt, K.R., Gaza, S., Voropaev, A., Ertl, S., Tiehm, A., 2014. Aerobic biodegradation of
1417 trichloroethene without auxiliary substrates. Water Res. 59 112−118.

1418 Sela-Adler, M., Ronen, Z., Herut, B., Antler, G., Vigderovich, H., Eckert, W., Sivan, O., 2017. Co-
1419 existence of methanogenesis and sulfate reduction with common substrates in sulfate-rich estuarine
1420 sediments. Front. Microbiol. DOI: 10.3389/fmicb.2017.00766.

1421 Semprini, L., Hopkins, G.D., McCarty, P.L., 1994. A field and modeling comparison of in situ
1422 transformation of trichloroethylene by methane utilizers and phenol utilizers. Lewis Publishers, Boca
1423 Raton, pp. 284–254.

1424 Seyedabbasi, M.A., Newell, C.J., Adamson, D.T., Sale, T.C., 2012. Relative contribution of DNAPL
1425 dissolution and matrix diffusion to the long-term persistence of chlorinated solvent source zones. J.
1426 Contam. Hydrol. 134 69–81.

1427 Sharma, P.K., McCarty, P.L., 1996. Isolation and characterization of a facultatively aerobic bacterium
1428 that reductively dehalogenates tetrachloroethene to cis-1,2-dichloroethene. Applied and Environ.
1429 Microbiol. 62 (3) 761−765.

1430 Shelley, F., Abdullahi, F., Grey, J., Trimmer, M., 2015. Microbial methane cycling in the bed of a chalk
1431 river: oxidation has the potential to match methanogenesis enhanced by warming. Freshwater Biol. 60
1432 (1) 150−160.

1433 Shim, H., Ryoo, D., Barbieri, P., Wood, T.K., 2001. Aerobic degradation of mixtures of
1434 tetrachloroethylene, trichloroethylene, dichloroethylenes, and vinyl chloride by toluene-o-xylene
1435 monooxygenase of *Pseudomonas stutzeri* OX1. Appl. Microbiol. Biotechnol. 56 (1) 265–269.

1436 Sieber, J.R., Le, H.M., McInerney, M.J., 2014. The importance of hydrogen and formate transfer for
1437 syntrophic fatty, aromatic and alicyclic metabolism. Environ. Microbiol. 16 (1) 177–188.

1438 Sieber, J.R., Sims, D.R., Han, C., Kim, E., Lykidis, A., Lapidus, A.L., McDonnald, E., Rohlin, L.,
1439 Culley, D.E., Gunsalus, R., McInerney, M.J., 2010. The genome of Syntrophomonas wolfei: new
1440 insights into syntrophic metabolism and biohydrogen production. Environ. Microbiol. 12 (8), 2289–
1441 2301.

1442 Simsir, B., Yan, J., Im, J., Graves, D., Löffler, F.E., 2017. Natural attenuation in streambed sediment

1443 receiving chlorinated solvents from underlying fracture networks. Environ. Sci. Technol. 51 (9) 4821–

1444 4830.

1445 Smidt, H., de Vos, W.M., 2004. Anaerobic microbial dehalogenation. Ann. Rev. Microbiol. 58 43−73.

1446 Sobczak, W.V., Findlay, S., 2002. Variation in bioavailability of dissolved organic carbon among stream

1447 hyporheic flowpaths. Ecology 83 (11) 3194–3209.

1448 Sonne, A.T., McKnight, U. S., Rønde, V., Bjerg, P.L., 2017. Assessing the chemical contamination

1449 dynamics in a mixed land use stream system. Water Research DOI: 10.1016./j.watres.2017.08.031.

1450 Squillace, P.J., Moran, M.J., 2007. Factors associated with sources, transport, and fate of volatile organic

1451 compounds and their mixtures in aquifers of the United States. Environ. Sci. Technol. 41 (7) 2123–

1452 2130.

1453 Stegen, J.C., Fredrickson, J.K., Wilkins, M.J., Konopka, A.E., Nelson, W.C., Arntzen, E.V., Chrisler,

1454 W.B., Chu, R.K., Danczak, R.E., Fansler, S.J., Kennedy, D.W., 2016. Groundwater-surface water

1455 mixing shifts ecological assembly processes and stimulates organic carbon turnover. Nat. Commun. 7:

1456 11237.

1457 Stelzer, R.S., Scott, J.T., Bartsch, L.A., Parr, T.B., 2014. Particulate organic matter quality influences

1458 nitrate retention and denitrification in stream sediments: evidence from a carbon burial experiment.

1459 Biogeochemistry 119 (1-3) 387−402.

1460 Storey, R.G., Fulthorpe, R.R., Williams, D.D., 1999. Perspectives and predictions on the microbial

1461 ecology of the hyporheic zone. Freshwater Biol. 41 (1), 119–130.

1462 Sung, Y., Fletcher, K.E., Ritalahti, K.M., Apkarian, R.P., Ramos-Hernández, N., Sanford, R.A.,

1463 Mesbah, N.M., Löffler, F.E., 2006. *Geobacter lovleyi* sp. nov. strain SZ, a novel metal-reducing and

1464 tetrachloroethene-dechlorinating bacterium. Appl. Environ. Microbiol. 72 (4) 2775−2782.

1465 Suttinun, O., Luepromchai, E., Müller, R., 2013. Cometabolism of trichloroethylene: concepts,

1466 limitations and available strategies for sustained biodegradation. Rev. Environ. Sci. Biotechnol. 12 (1)

1467 99–114.

1468   Sutton, N.B., Atashgahi, S., Saccenti, E., Grotenhuis, T., Smidt, H., Rijnaarts, H.H.M., 2015. Microbial

1469   community response of an organohalide respiring enrichment culture to permanganate oxidation. PLoS

1470   One 10: e0134615.

1471   Tan, K., Anderson, T.A., Jackson, W.A., 2005. Temporal and spatial variation of perchlorate in

1472   streambed sediments: results from in-situ dialysis samplers. Environ. Pollut. 136 (2) 283–291.

1473   Taş, N., van Eekert, M.H., Wagner, A., Schraa, G., de Vos, W.M., Smidt, H., 2011. Role of

1474   "Dehalococcoides" spp. in the anaerobic transformation of hexachlorobenzene in European rivers. Appl.

1475   Environ. Microbiol. 77 (13) 4437−4445.

1476   Ter Meer, J., Gerritse, J., Di Mauro, C., Harkes, M.P., Rijnaarts, H.H.M., Cinjee, A.C., van Liere, I.H.,

1477   Slenders, I.H., Baartmans, R.F.W., 1999. Hydrogen as indicator for in-situ redox condition and

1478   dechlorination. Natural Attenuation of Environmental Contaminants, TNO-MEP R 99/341. TNO

1479   Institute of Environmental Sciences, Energy Research and Process Innovation, The Netherlands, pp.1-

1480   125.

1481   Tiehm, A., Schmidt, K.R., 2011. Sequential anaerobic/aerobic biodegradation of chloroethenes—

1482   aspects of field application. Curr. Opin. Biotechnol. 22 (3) 415−421.

1483   Tiehm, A., Schmidt, K.R., Pfeifer, B., Heidinger, M., Ertl, S., 2008. Growth kinetics and stable carbon

1484   isotope fractionation during aerobic degradation of cis-1, 2-dichloroethene and vinyl chloride. Water

1485   Res. 42 (10) 2431−2438.

1486   Trauth, N., Schmidt, C., Vieweg, M., Maier, U., Fleckenstein, J.H., 2014. Hyporheic transport and

1487   biogeochemical reactions in pool-riffle systems under varying ambient groundwater flow conditions. J.

1488   Geophys. Res. Biogeosci. 119 (5) 910–928.

1489   Trauth, N., Schmidt, C., Vieweg, M., Oswald, S.E., Fleckenstein, J.H., 2015. Hydraulic controls of

1490   in-stream gravel bar hyporheic exchange and reactions. Water Resour. Res. 51 (4) 2243−2263.

1491   Trimmer, M., Maanoja, S., Hildrew, A.G., Pretty, J.L., Grey, J., 2010. Potential carbon fixation via

1492   methane oxidation in well-oxygenated riverbed gravels. Limnol. Oceanogr. 55 (2) 560.

1493   Tristram, D.A., Krause, S., Levy, A., Robinson, Z.P., Waller, R.I., Weatherill, J.J., 2014. Identifying

1494   spatial and temporal dynamics of proglacial groundwater–surface-water exchange using combined

1495   temperature-tracing methods. Freshwater Sci. 34 (1) 99–110.

1496   Ullah, S., Zhang, H., Heathwaite, A.L., Binley, A., Lansdown, K., Heppell, K., Trimmer, M., 2012. In

1497   situ measurement of redox sensitive solutes at high spatial resolution in a riverbed using diffusive

1498   equilibrium in thin films (DET). Ecol. Eng. 49 18–26.

1499   Ullah, S., Zhang, H., Heathwaite, A.L., Heppell, C., Lansdown, K., Binley, A., Trimmer, M., 2014.

1500   Influence of emergent vegetation on nitrate cycling in sediments of a groundwater-fed river.

1501   Biogeochemistry 118 (1-3) 121−134.

1502   Vandermeeren, P., Herrmann, S., Cichocka, D., Busschaert, P., Lievens, B., Richnow, H.H., Springael,

1503   D., 2014. Diversity of dechlorination pathways and organohalide respiring bacteria in chlorobenzene

1504   dechlorinating enrichment cultures originating from river sludge. Biodegradation 25 (5) 757–776.

1505   Vannelli, T.O.D.D., Logan, M.Y.K.E., Arciero, D.M., Hooper, A.B., 1990. Degradation of halogenated

1506   aliphatic compounds by the ammonia-oxidizing bacterium *Nitrosomonas europaea*. Appl. Environ.

1507   Microbiol. 56 (4) 1169–1171.

1508   Verce, M.F., Ulrich, R.L., Freedman, D.L., 2000. Characterization of an isolate that uses vinyl chloride

1509   as a growth substrate under aerobic conditions. Appl. Environ. Microbiol. 66 (8) 3535−3542.

1510   Verce, M.F., Ulrich, R.L., Freedman, D.L., 2001. Transition from cometabolic to growth-linked

1511   biodegradation of vinyl chloride by a *Pseudomonas* sp. isolated on ethene. Environ. Sci. Technol. 35

1512   (21) 4242−4251.

1513   Vidon, P.G., Hill, A.R., 2004. Landscape controls on nitrate removal in stream riparian zones. Water

1514   Resour. Res. 40 (3) W03201.

1515   Vieweg, M., Kurz, M.J., Trauth, N., Fleckenstein, J.H., Musolff, A., Schmidt, C., 2016. Estimating

1516   time-variable aerobic respiration in the streambed by combining electrical conductivity and dissolved

1517   oxygen time series. J. Geophys. Res. Biogeosci. 121 (8) 2199−2215.

1518 Vogel, T.M., Criddle, C.S., McCarty, P.L., 1987. Transformation of halogenated aliphatic compounds.

1519 Environ. Sci. Technol. 21 (8) 722−736.

1520 Voisin, J., Cournoyer, B., Mermillod-Blondin, F., 2016. Assessment of artificial substrates for

1521 evaluating groundwater microbial quality. Ecol. Indic. 71 577–586.

1522 Wackett, L.P., Gibson, D.T., 1988. Degradation of trichloroethylene by toluene dioxygenase in whole-

1523 cell studies with *Pseudomonas putida* F1. Appl. Environ. Microbiol. 54 (7) 1703–1708.

1524 Wagner, D.D., Hug, L.A., Hatt, J.K., Spitzmiller, M.R., Padilla-Crespo, E., Ritalahti, K.M., Edwards,

1525 E.A., Konstantinidis, K.T., Löffler, F.E., 2012. Genomic determinants of organohalide-respiration in

1526 *Geobacter lovleyi*, an unusual member of the *Geobacteraceae*. BMC Genomics 13 (1) 200.

1527 Walker, C.B., He, Z., Yang, Z.K., Ringbauer, J.A., He, Q., Zhou, J., Voordouw, G., Wall, J.D., Arkin,

1528 A.P., Hazen, T.C., Stolyar, S., 2009. The electron transfer system of syntrophically grown *Desulfovibrio*

1529 *vulgaris*. J. Bacteriol. 191 (18) 5793–5801.

1530 Wang, G., Allen-King, R.M., Choung, S., Feenstra, S., Watson, R., Kominek, M., 2013. A practical

1531 measurement strategy to estimate nonlinear chlorinated solvent sorption in low foc sediments.

1532 Groundwater Monit. Remediat. 33 (1) 87 – 96.

1533 Weatherill, J. J., 2015. Investigating the natural attenuation and fate of a trichloroethene plume at the

1534 groundwater-surface water interface of a UK lowland river. PhD thesis, School of Physical and

1535 Geographical Sciences, Keele University, UK.

1536 Weatherill, J., Krause, S., Voyce, K., Drijfhout, F., Levy, A., Cassidy, N., 2014. Nested monitoring

1537 approaches to delineate groundwater trichloroethene discharge to a UK lowland stream at multiple

1538 spatial scales. J. Contam. Hydrol. 158 38–54.

1539 Wei, N., Finneran, K.T., 2011. Influence of ferric iron on complete dechlorination of trichloroethylene

1540 (TCE) to ethene: Fe (III) reduction does not always inhibit complete dechlorination. Environ. Sci.

1541 Technol. 45 (17) 7422−7430.

1542 Wei, N., Finneran, K.T., 2013. Low and high acetate amendments are equally as effective at promoting

1543 complete dechlorination of trichloroethylene (TCE). Biodegradation 24 (3) 413−425.

1544   Wiedemeier, T.D.H., Swanson, M.A., Moutoux,D.E., Gordon,K., Wilson, J.T., Wilson, B.H., Kampbell,

1545   D.H., Haas, P.E., Miller, R.N., Hansen, J.E., Chapelle, F.H., 1998. Technical Protocol for Evaluating

1546   Natural Attenuation of Chlorinated Solvents in Ground Water, IAG: RW57936164. US Environmental

1547   Protection Agency, USA.

1548   Wilson, F. P., Liu, X., Mattes, T. E., Cupples, A. M., 2016. *Nocardioides*, *Sediminibacterium*,

1549   *Aquabacterium*, *Variovorax*, and *Pseudomonas* linked to carbon uptake during aerobic vinyl chloride

1550   biodegradation. Environ. Sci. Pollut. Res. 23 (19) 19062−19070.

1551   Wittlingerová, Z., Macháčková, J., Petruželková, A., Zimová, M., 2016. Occurrence of

1552   perchloroethylene in surface water and fish in a river ecosystem affected by groundwater contamination.

1553   Environ. Sci. Pollut. Res. 23 (6) 5676–5692.

1554   Woessner, W.W., 2000. Stream and fluvial plain ground water interactions: rescaling hydrogeologic

1555   thought. Ground Water, 38 (3) 423–429.

1556   Wondzell, S.M., 2011. The role of the hyporheic zone across stream networks. Hydrol. Process. 25 (22)

1557   3525–3532.

1558   Wu, H., Chen, X.P., Liu, G.P., Jiang, M., Guo, T., Jin, W.Q., Wei, P., Zhu, D.W., 2012. Acetone–

1559   butanol–ethanol (ABE) fermentation using *Clostridium acetobutylicum* XY16 and in situ recovery by

1560   PDMS/ceramic composite membrane. Bioprocess Biosyst. Eng. 35 (7) 1057–1065.

1561   Yager, R.M., Bilotta, S.E., Mann, C.L., Madsen, E.L., 1997. Metabolic adaptation and in situ attenuation

1562   of chlorinated ethenes by naturally occurring microorganisms in a fractured dolomite aquifer near

1563   Niagara Falls, New York. Environ. Sci. Technol. 31 (11) 3138−3147.

1564   Yang, M., Annable, M.D., Jawitz, J.W., 2014. Back diffusion from thin low permeability zones.

1565   Environ. Sci. Technol. 49 (1) 415–422.

1566   Yang, Y., Higgins, S.A., Yan, J., Şimşir, B., Chourey, K., Iyer, R., Hettich, R.L., Baldwin, B., Ogles,

1567   D.M., Löffler, F.E., 2017. Grape pomace compost harbors organohalide-respiring Dehalogenimonas

1568   species with novel reductive dehalogenase genes. ISME J. DOI:10.1038/ismej.2017.127.

1569 Yang, Y., McCarty, P.L., 1998. Competition for hydrogen within a chlorinated solvent dehalogenating

1570 anaerobic mixed culture. Environ. Sci. Technol. 32 (22) 3591−3597.

1571 Yu, H.Y., Wang, Y.K., Chen, P.C., Li, F.B., Chen, M.J., Hu, M., Ouyang, X., 2014. Effect of nitrate

1572 addition on reductive transformation of pentachlorophenol in paddy soil in relation to iron (III)

1573 reduction. J. Environ. Manage. 132 42−48.

1574 Yu, S., Dolan, M.E., Semprini, L., 2005. Kinetics and inhibition of reductive dechlorination of

1575 chlorinated ethylenes by two different mixed cultures. Environ. Sci. Technol. 39 (1) 195−205.

1576 Yu, Z., Smith, G.B., 2000. Inhibition of methanogenesis by C1-and C2-polychlorinated aliphatic

1577 hydrocarbons. Environ. Toxicol. Chem. 19 (9) 2212−2217.

1578 Zarnetske, J.P., Haggerty, R., Wondzell, S.M., Baker, M.A., 2011. Labile dissolved organic carbon

1579 supply limits hyporheic denitrification. J. Geophys. Res. Biogeosci. 116 G04036.

1580 Zarnetske, J.P., Haggerty, R., Wondzell, S.M., Bokil, V.A., González-Pinzón, R., 2012. Coupled

1581 transport and reaction kinetics control the nitrate source-sink function of hyporheic zones. Water Resour.

1582 Res. 48 (11) W11508.

1583 Ziv-El, M., Popat, S.C., Cai, K., Halden, R.U., Krajmalnik-Brown, R., Rittmann, B.E., 2012. Managing

1584 methanogens and homoacetogens to promote reductive dechlorination of trichloroethene with direct

1585 delivery of H_2 in a membrane biofilm reactor. Biotechnol. Bioeng. 109 (9) 2200−2210.

1586 **Fig. 1.** Generic conceptual model of a groundwater CE plume discharging through heterogeneous

1587 hyporheic zone sediments with a range of solute residence times. The plume may be composed of HCEs,

1588 LCEs or a mixture of both. Dashed line indicates the approximate boundary between an upper oxic zone

1589 and lower suboxic/anoxic zone induced by buried sedimentary organic matter. OM: organic matter; K:

1590 sediment hydraulic conductivity. Brown areas in inset circles represents buried sedimentary organic

1591 matter (adapted from Gomez-Velez et al., 2014).

1592 **Fig. 2.** Schematic representation of hyporheic zone electron flow derived from complex organic matter

1593 metabolism (adapted from Heimann et al., 2009) to organohalide-respiring bacterial communities in

1594 anoxic riverbed sediments. Processes depicted include: orange arrow: hydrolysis; green arrows:

1595 fermentation; brown arrows: carbon assimilation; dashed red arrow: ammonification; dashed green

1596 arrow: methanogensis; blue arrows/lines: electron transport and red arrows: organohalide respiration.

1597 Ac: acetate; DIC: dissolved inorganic carbon; ETH: ethene. Representative Gibb's free energy ($\Delta G°$)

1598 values (kJ/M) indicated for sequential reduction of PCE to ethene taken from Dolfing and Beurskens

1599 (1995) with representative Eh values from Wiedemeier et al. (1998) under standard conditions reported

1600 therein.

1601 **Fig. 3.** Influence of extracellular hydrogen concentrations on growth rates of fermenters and

1602 hydrogenotrophs (redrawn from Ter Meer et al., 1999).

1603 **Fig. 4.** Idealised ecological succession of terminal electron acceptors and their reduced metabolites in

1604 hyporheic zones based on observed molecular hydrogen (H_2) threshold concentrations. Ac: acetate;

1605 ETH: ethene. Gibb's free energy ($\Delta G°$) values (kJ/M) from Heimann et al. (2009) with representative

1606 Eh values from Wiedemeier et al. (1998) under standard conditions reported therein. Observed minimum

1607 hydrogen threshold ranges: (1) Cord-Ruwish et al. (1988); (2) Haring et al. (1991); (3) Sung et al. (2006);

1608 (4) Lu et al. (2001); (5) Mazur et al. (2001); (6) Lovely et al. (1989); (7) Caccavo et al. (1992); (8)

1609 Luijten et al. (2004); (9) Lovely et al. (1985).

1610 **Fig. 5.** (a) Conceptual illustration of potential metabolic (black arrows) and co-metabolic mineralisation

1611 of cDCE and VC (red arrows) at the dispersive mixing zone between upwelling anoxic groundwater

1612 containing DOM by-products (ammonium and methane) and oxic hyporheic flow cells (blue arrows).

1613   DIC: dissolved inorganic carbon; ETH: ethene. Note that reactive intermediates from co-metabolism are

1614   omitted for clarity. (b) Numerical simulations of oxygen concentration and uptake rate under gaining

1615   flow conditions in a dune bedform (adapted from Trauth et al., 2014). (c) Simulation of bedform mixing

1616   zone thickness with varying sediment hydraulic conductivity (K) and vertical groundwater flux (q_z)

1617   using a conservative groundwater tracer dilution approach (adapted from Hester et al., 2013).

1618   **Fig. 6.** Vertical pore water chemical gradients from selected case studies illustrating a range of in-situ

1619   transformation capacities (refer to Table 1 for profile context and supporting information). Black

1620   diamonds: TCE; open squares: cDCE; open triangles: VC; green circles: ethane; blue circles: ethane;

1621   orange squares: methane. Redrawn from: (a) Weatherill et al. (2014); (b) Abe et al. (2009); (c) Freitas

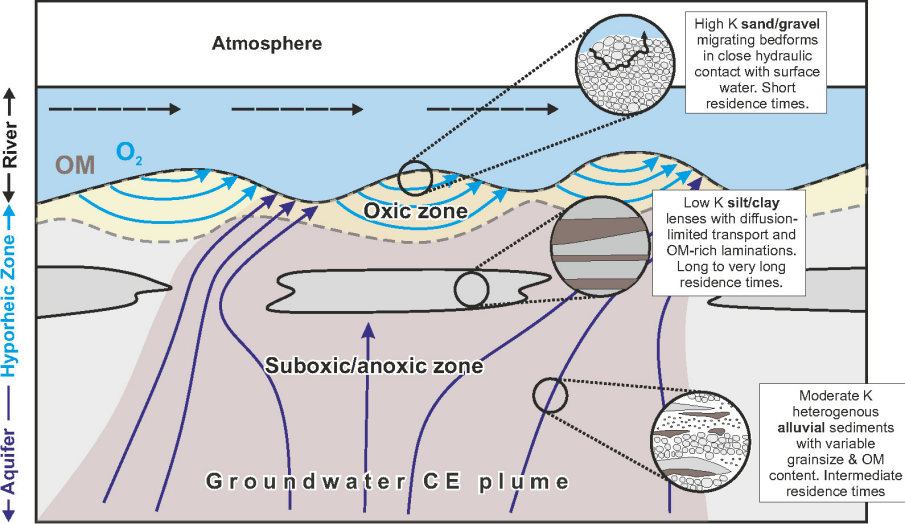1622   et al. (2015) and (d) Simsir et al. (2017).

Table 1: Field experience of chlorinated ethene plume discharging to surface water receptors illustrating a range of in-situ transformation potentials from selected case studies (continued overleaf).
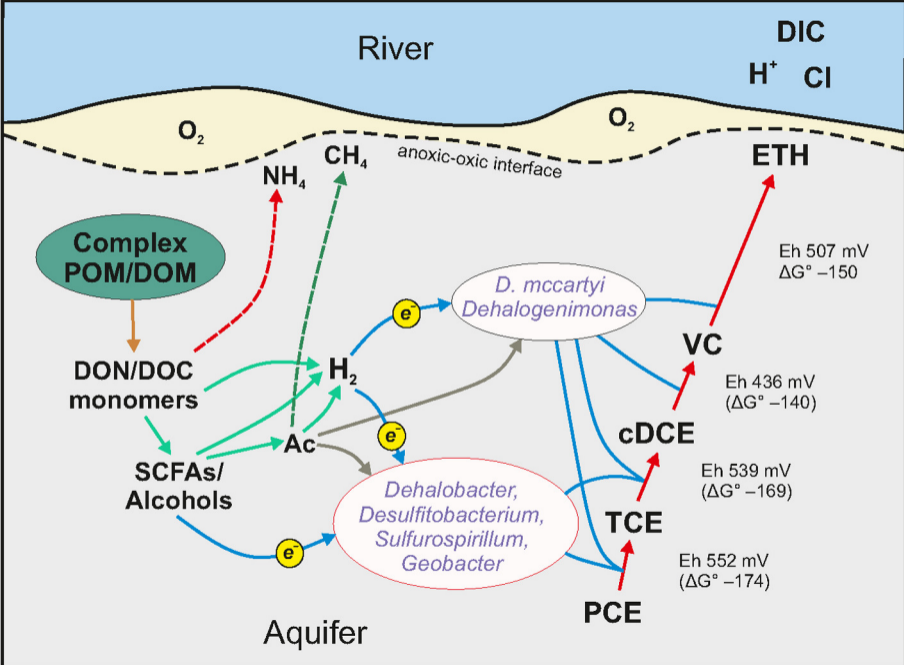
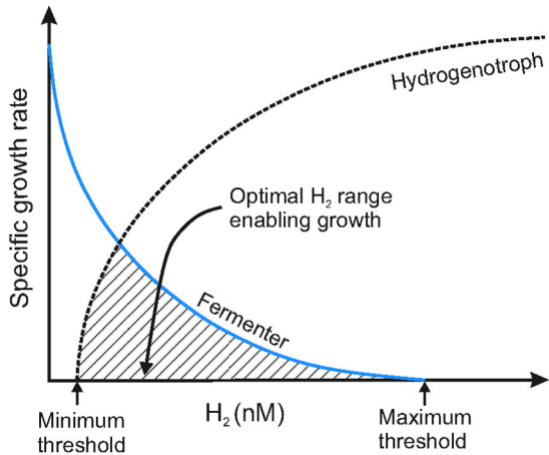| Receptor	CE source	Aquifer	Plume	Mass flux to surface water (kg/y)	Residence time (d/m)	In-situ biotransformation potential	References
Grindsted Stream, Jutland, Denmark.	Pharmaceutical factory in operation from 1914 to 1999.	Quaternary and Tertiary sands, underlain by thick regional clay layer, natural gradients.	cDCE (47 µM) and VC (72 µM). Co-mingled hydrocarbons.	45–123 (cDCE), 42–123 (VC)	0.4–10	**Low**, although not specifically addressed. CE-impacted stream, also impacted by metals and other organic contaminants.	Rønde et al., 2017; Sonne et al., 2017.
Third Creek, Knoxville, Tenessee, USA.	Spills associated with historic metal processing facility operated for over a century.	Fractured/karstic dolomite. Overlain by silty-clay saprolite, natural gradients.	PCE and TCE (6-60 µM). Co-mingled 1,1,1-TCA, TCM, hydrocarbons.	16.1 (TCE + cDCE)	58	**High.** No CEs detectable in surface water. Stochiometric cDCE transformation in SO_4-reducing conditions and potential CH_4 cometabolism. Hydrocarbon co-contamiants source of SCFAs. Well distributed *D. mccartyi* population.	Simsir et al., 2017.
River Tame, Birmingham, UK.	Multiple historic urban/industrial sources, City of Birmingham.	Unconfined Permo-Triassic sandstones. Complex urban environment. Gradients historically affected by abstractions.	TCE + cDCE (0.25–9.5 µM). Measured in riverbed piezometers.	20–200 (TCE) over 7.4 km city reach	12–100 (sorption modified)	**Transiently high**, low-moderate overall. Stochiometric TCE transformation to ethene in riffle sequence under Mn(IV) reduction. HEF and buried SOM a source of DOC driving redox. Inhibition by high SO_4 (5 mM) suspected.	Freitas et al., 2015; Roche et al., 2009; Ellis and Rivett, 2007.

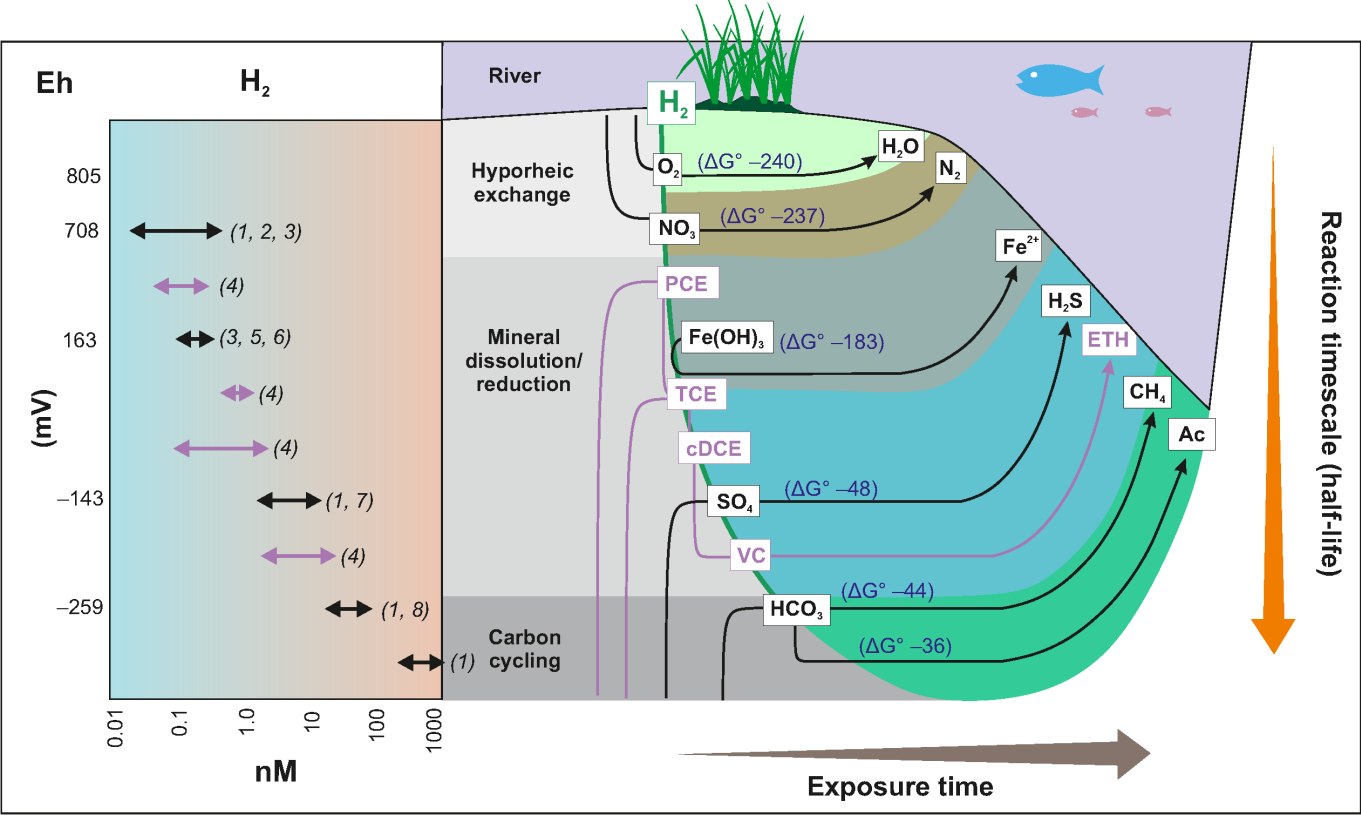|							
Zenne River, Vilvoorde, Belgium	Multiple industrial sources, Vilvoorde area.	Unconfined superficial gravel aquifer in urban setting. Gradients affected by retaining walls and canal water seepage.	VC (35 µM), cDCE (12 µM). 1.4 km wide plume.	Not addressed.	12–29	**High**. Transformation of cDCE and VC in up to 75% of locations. SOM-enriched sediments due to eutrophic conditions. *D. mccartyi* populations associated with SOM. VC/Ethene oxidisers present in SOM-poor zones.	Hamonts et al., 2009; 2012; Atashgahi et al., 2013; 2017a.
River Tern, Shropshire, UK.	Unknown. Suspected to be associated with a millitary airfield 1.5 km away.	Unconfined Permian sandstone. Natural gradients, occasional abstractions, agricultural setting.	TCE (0.1–1.4 µM).	0.15–0.55 (TCE)	0.5–1081 (sorption modified)	**Low** to **moderate** (patchy). Mass flux dominated by preferential pathways. Local TCE to cDCE hotspots associated peat lenses and surficial sediments. Elevated NO_3 in aerobic aquifer.	Weatherill et al., 2014; Weatherill, 2015.
Skensved Stream, Sjaelland, Denmark.	Leaking TCE storage tank, auto lacquer shop in operation since 1974. Leak discovered in 1993.	Interbedded soil, sand and gravel overlying bryozoan limestone. Pump-and-treat plume control in operation.	Max TCE (0.9 µM)	33 (TCE modelled from DNAPL source)	Not addressed	**Low,** aerobic to denitrifying conditions in hyporheic zone. Stream CE impact controlled by pump-and-treat system (as of 2009).	McKnight et al., 2010.
Pine River, Ontario, Canada.	Dry cleaning facility 195 m from river. PCE DNAPL contamination originated in the 1970s.	Semi-confined interbedded sand and clays in urban setting. Natural gradients.	Max PCE (0.25 mM)	3–53 (PCE) during 1995-1999.	858–71175 (sorption modified in silt/clay). Locally 3–23.	**High.** 52% of plume transformed to cDCE in riverbed. Stoichiometric ethene production in Fe(III)/SO_4 reducing SOM zones supporting *D. mccartyi* populations . Widespread aerobic VC mineralisation potential.	Conant et al., 2004; Abe et al., 2009.
Little Bayou Creek, McCracken County, Kentucky, USA.	Uranium enrichment facility, TCE used from 1953 to1996 for cleaning. Residual DNAPL volume of 795 m^3.	Regional gravel aquifer locally confined by silt and clay. Channelised river flow regime.	TCE near solubility limit near source (8.4 mM). 0.12–13 µM in riverbed. Co-mingled [99]Tc.	3-57 (TCE)	Not addressed	**Low**, TCE impacted surface water. No LCEs detectable in aerobic riverbed conditions with high mass flux through springs. Strong seasonal variability in stream water TCE concentrations.	LaSage et al., 2008; Fryar et al., 2000.

| Unnamed Triburatary Streams, Industrial Facility, Conneticut, USA. | Manufacturing facility, 1970s underground degreaser tanks. TCE DNAPL source isolated in 1994. Plumes sustained by back-diffusion. | Unconfined surficial aquifer underlain by extensive aquitard. Steep topography, visible groundwater seepage zones. | TCE (18–24 μM), cDCE (5 μM) at Transect 2. | 10 (TCE + cDCE) from Transect 2. | Not addressed | **Unknown.** Hyporheic zone processes in the streambeds not specifically investigated. | Chapman et al., 2007. |

Atmosphere

River — Hyporheic Zone — Aquifer

OM   O$_2$

Oxic zone

Suboxic/anoxic zone

Groundwater CE plume

High K **sand/gravel** migrating bedforms in close hydraulic contact with surface water. Short residence times.

Low K **silt/clay** lenses with diffusion-limited transport and OM-rich laminations. Long to very long residence times.

Moderate K heterogenous **alluvial** sediments with variable grainsize & OM content. Intermediate residence times

Specific growth rate (y-axis)

H₂ (nM) (x-axis)

Hydrogenotroph

Optimal H₂ range enabling growth

Fermenter

Minimum threshold

Maximum threshold

(a)

O₂ → Atmosphere

Surface Water

DIC
NO₂ Cl

Aerobic respiration

Mixing zone

ETH

Complex POM/DOM NH₄ CH₄ VC

DON/DOC monomers SCFAs/Alcohols cDCE

Anaerobic respiration

(b)

O₂ mM

0.3 0.2 0.1 0

O₂ uptake mM/L/d

0.4 0.2 0

(c)

Groundwater Tracer

0 3 6 9
mg/L

K = 25 m/d   q_z = 0.55 m/d

K = 84.4 m/d   q_z = 1.09 m/d

K = 150 m/d   q_z = 5.47 m/d

(a) **River Tern**, Shropshire, UK
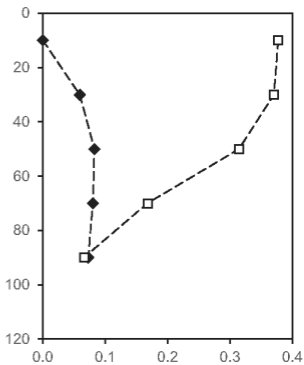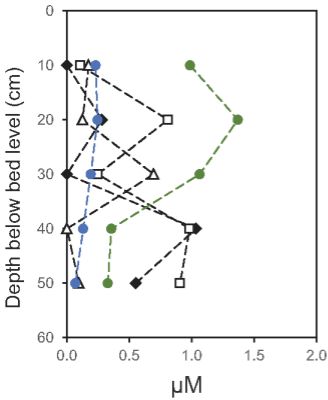
(b) **Pine River**, Ontario, Canada

(c) **River Tame**, Birmingham, UK.

(d) **Third Creek**, Tennessee, US.